ON THE INFLUENCE OF WALL BOUNDARY LAYERS IN CLOSED TRANSONIC TEST SECTIONS

Thesis by

Sune B. Berndt

In Partial Fulfillment of the Requirements

for the Degree of

Doctor of Philosophy

California Institute of Technology

Pasadena, Califonia

1955

A C K N O W L E D G M E N T S

The writer wishes to acknowledge his deep indebtedness to Professors J. Cole, A Erdelyi, P. Lagerstrom, H. Liepmann and K. Oswatitsch for inspiring teaching and stimulating discussions on topics related to fluid mechanics in general and to the theory of transonic flow in particular. He found their generous attitude most encouraging.

To many other persons are thanks due for valuable discussions and helpful advice. The writer would like to mention here Professor L. Lees of this Institute and Messrs. Drougge and Petersohn of the Aeronautical Research Institute of Sweden (FFA).

Finally, he wishes to thank the Director of the FFA for permission to include in this thesis material worked out while the writer was an employee of the FFA. This research was also partially supported by the Office of Scientific Research under Contract AF-18 (600)-383 with the Air Research and Development Command.

ABSTRACT

The boundary layers at the test section walls of a transonic wind tunnel are known to reduce the wall interference. In the present paper this effect is studied by means of small perturbation theory, assuming viscosity to be negligible when perturbing a turbulent boundary layer. An approximation for thin boundary layers leads to a modified boundary condition at the wall of the test section, expressing the normal streamline slope induced by changes in mass flow density and crossflow within the boundary layer. This boundary condition is applied to the linearized equations of subsonic flow and to the non-linear transonic equations at choking, the cases of plane and circular test sections only being treated in detail.

The results of linear theory show that all corrections except the three-dimensional angle-of-attack correction are considerably reduced by the presence of the boundary layers at Mach numbers greater than 0.9, the essential part of their influence being due to the change of mass flow density with pressure. In the case of choking the analysis indicates that the presence of boundary layers will increase the maximum model size for which the flow can be interpreted as corresponding to Mach number one in free flight. Finally, the technique of using artificial thickening of the wall boundary layers for reduction of wall interference is considered, though without reaching a definite conclusion as to its value compared to other techniques.

TABLE OF CONTENTS

I. INTRODUCTION

1.1 The experimental background

Wall interference in the closed test section of a wind tunnel constitutes a severe limitation to the model size at high subsonic Mach numbers. For a given model size there is a largest attainable Mach number in front of the model, the choking Mach number, which is smaller than one. The highest Mach number at which measured data can be corrected for wall interference is still smaller. Even for very small models, to the standards of low speed and supersonic tests, there is a Mach number range where the wall corrections are large, complicated to compute and not even well defined (References 1 and 2).

Recently it was noted by Petersohn (Reference 3) that the boundary layers at the walls of the test section might contribute to the wall interference at high subsonic Mach numbers. By artificially thickening the boundary layers of a given test section he demonstrated that they work to decrease the wall interference and to increase the choking Mach number. It was evident from the tests that the effect might be considerable at Mach numbers close to the choking Mach number, and that there is no essential difference in this respect between the flow about two-dimensional profiles and the flow about bodies of small aspect ratio. Petersohn suggested that the artificial thickening of the boundary layers could be systematically used as a means of reducing the wall interference.

Although the effect found was rather strong considering the comparatively thin boundary layers investigated, its existence and general character should not surprise. The following argument used in Reference 3 is enlightening. When the wall boundary layer is very thick the situation is much like that for an open test section. It is well known that in this case the blockage

correction, say, is of the same magnitude but of opposite sign as for a closed test section of the same form - if only the corrections exist and can be calculated from linear theory. Hence one concludes, assuming continuity and monotony, that thin boundary layers should reduce the correction, and that for some boundary layer thickness there should by no correction at all.

A somewhat deeper insight might be obtained from the following reasoning. The wall interference may be thought of as caused by the walls straightening the streamlines of the unbounded flow. Following the flow along an undisturbed streamline (assuming subsonic speed) at the locus of the wall one first moves away from the model in a region of decreasing pressure and then approaches the model in a region of increasing pressure. The important point now is that a given pressure change produces a larger relative change of mass flow density within the boundary layer than just outside it, since the boundary layer flow at an average is farther from the maximum of mass flow density corresponding to sonic velocity. As a result there is a displacing effect of the boundary layer for increasing pressure and conversely for decreasing pressure. The pressure distribution at the wall has essentially the same form as in unbounded flow, and hence it is seen that the wall boundary layers tend to reduce the straightening effect of the wall and to produce a streamline shape similar to that of unbounded flow. Thus a reduction of the wall influence should be expected from the boundary layers.

From essentially the same argument it was concluded by Oswatitsch in Reference 4 that strong boundary layer effects are likely to occur at transonic speeds[+]. He suggested that in many cases one would not be able to apply the classical iteration procedure - where the displacement effect of the boundary layer is computed from an approximate pressure field and used to compute a

---

[+]Several other authors have discussed this point, generally in connection with the problem of shock-wave boundary-layer interaction or the problem of shock-free locally supersonic flow.

new pressure field etc. - but that the equations for the outer flow field and the boundary layer would have to be solved simultaneously. He showed that the flow field in the throat of a Laval nozzle is influenced by the boundary layers, and estimated this influence by application of one-dimensional theory and a simple hypothesis for the variation of the displacement thickness with free stream velocity. In addition to the principal aspects, this case is of specific interest in the present context since the flow field in question is very similar to that about a large model at choking (see also Reference 5).

1.2 The boundary layer perturbation problem

The problem of relating in a simple but adequate manner the displacement effect of the boundary layer to the pressure perturbation due to the model evidently is of basic importance for the understanding of the wall boundary layer influence. The present study will treat only such cases where the model is situated far from the walls. It is then thought sufficient to consider only the following restricted problem: to determine the small perturbation of a given stable boundary layer caused by a steady pressure perturbation acting over a length which is small compared to the upstream length of the boundary layer.

The models used for transonic tests in closed test sections are necessarily small, and in addition they usually are slender. Thus the pressure perturbation at the wall is small and so is the boundary layer perturbation except where shock waves reach the wall. In the latter case, however, the influence is felt only in a downstream region which is likely to be completely behind the region of dependence of the model. Furthermore, it is characteristic for transonic fields that perturbations penetrate not very far in the upstream direction. Consequently the pressure perturbation at the wall starts not very

far ahead of the model, and only such boundary layer perturbations, as occur closely behind or in front of the rear end of the model, contribute much to the boundary layer influence at the model. The length of this critical region of the wall is expected to be small compared to the upstream length of the boundary layer except when the boundary layer is very thin[+].

These arguments in favor of considering only the restricted perturbation problem are of course rather crude, and they should be reconsidered in each specific case of application. Only if they are accepted, however, will the analysis be reasonably simple. The simplifications made possible are essentially the following:

(i) A linear perturbation theory may be used, except that a non-linear term of the transonic type might have to be kept.

(ii) The unperturbed boundary layer may be taken to have constant thickness independent of the streamwise coordinate.

(iii) Viscous effects may be neglected, except possibly in the immediate neighborhood of the wall.

The last point requires some clarification. When the boundary layer enters the perturbing pressure field (here we take a Lagrangian point of view), an acceleration field is set up which counteracts the pressure gradient. The perturbation of the viscous stress is not believed to contribute to the force balance until the velocity gradient has been essentially changed (that means a second order contribution), except in the immediate neighborhood of the wall, where the acceleration is forced to be small. The viscous stress (or rather the vorticity) produced at the wall diffuses into the boundary layer but will not penetrate it until further downstream, since the length required is of the order of the upstream length. The argument put forward is designed for the laminar case, but there is no obvious reason why it should not apply to the turbulent case as well.

[+]For an artificially thickened boundary layer a properly defined effective upstream length is understood to be used.

The simplifications (i), (ii) and (iii) are commonly introduced also when dealing with the very similar problem of weak shock-wave boundary-layer interaction, and many ideas can be taken over from the comprehensive literature on that problem. A rather complete and up to date survey of it was given in Reference 6 by Lighthill, and the close similarity of the two problems may be appreciated from comparing pertinent parts of that paper with the comment to point (iii) given above or with References 18 and 7, where the viscous effects close to the wall were investigated in some detail.

A simple case arises when viscosity is completely neglected. To permit this the boundary layer velocity distribution must not approach zero at the wall but a value which is not too small, compared to the free stream velocity. This is of course not a physically possible type of boundary layer, but it might be a reasonable approximation for turbulent boundary layers where the low-speed layer close to the wall is very thin.

For special Mach number profiles it is possible to find explicit solutions of the nonviscous linear perturbation problem. The most primitive choice is to take the Mach number to be constant within the boundary layer, as was done by Tsien and Finston (Reference 8) in the shock wave case. An application to the present problem was reported in Reference 9. The result was in qualitative agreement with experiments but left the question open how to correlate the discontinuous boundary layer with a real one. Earlier Vandrey (Reference 10) had studied by a similar method the use of discontinuities in the velocity distribution of the test section as a means of reducing wall interference.

An obvious source of information on the displacement effects of the wall boundary layer is boundary layer theory. It is fundamental for this theory that pressure is constant through the boundary layer, and consequent-

ly one has to restrict the application to cases where the thickness is sufficiently small compared to the size of the model and the test section. Oswatitsch in Reference 4 applied the Kármán momentum integral to a one-parameter family of laminar boundary layers, and thus derived an expression for the displacement thickness as a function of the velocity distribution outside the boundary layer. It was evident from the result that viscous effects contribute essentially. For the turbulent case he concluded on the other hand that viscosity is negligible, and sustained this by experimental evidence.

1.3 Outline of the present study

An investigation of the influence of wall boundary layers in transonic test sections should aim at the solution of the following two problems:

I. To what extent is the influence appreciable for those boundary layers which exist in current tunnels, and how can corrections be determined?

II. Is it possible to choose the wall boundary layers to give a considerable reduction of the wall interference, and how can the proper choice be accomplished?

The present study will not provide the answere. The problems are difficult to solve by analytical methods since a non-linear differential equation has to be used when the flow is transonic, and in the end one will have to resort to comprehensive experiments. The intention of the present study rather is to find out whether such an experimental investigation will be worth while or not, and to provide a basis for planning and interpreting the experiments.

Two restricted cases will be considered in some detail, namely the case when linearized theory is applicable and the case of choked flow. They correspond to the upper and lower bounds of the Mach number range in which

wall interference makes tests difficult in a closed test section. The problem for the intermediate part of the range, which is thought too complicated to be treated at this stage, will be discussed in the concluding chapter.

In both cases an approximation for thin boundary layers is used, which is essentially equivalent to that of boundary layer theory, although viscosity is neglected. In developing this approximation a somewhat broader attitude is taken than is strictly necessary for the present needs, the intention being to provide a basis for future study of less restricted problems. However, from the very beginning the influence of viscosity on the boundary layer perturbation is neglected, and the result consequently is applicable at most for turbulent boundary layers. Only under very special circumstances are the wall boundary layers likely to be laminar (as for example in Reference 11), so the restriction might not be serious.

II. EQUATIONS FOR TRANSONIC SHEAR FLOW

2.1 Basic assumptions

As was argued in the Introduction, the viscous stress is negligible in the essential part of the perturbation field set up by a slender model in the test section of a wind tunnel at transonic speeds. It is the purpose of the present chapter to derive the differential equations and the boundary conditions for that part of the field.

The test section is taken to be bounded by a cylindrical surface Γ, within which the unperturbed flow is everywhere parallel to the generators. We choose a Cartesian coordinate system Oxyz with the x-axis in the flow direction (see Figure 1). The Mach number M and density R are assumed to be constant along a given streamline. Thus they are functions of y and z only; we postulate them to have continuous first derivatives. The pressure has the same constant value P everywhere. The velocity distribution U(y,z) is determined by the formula

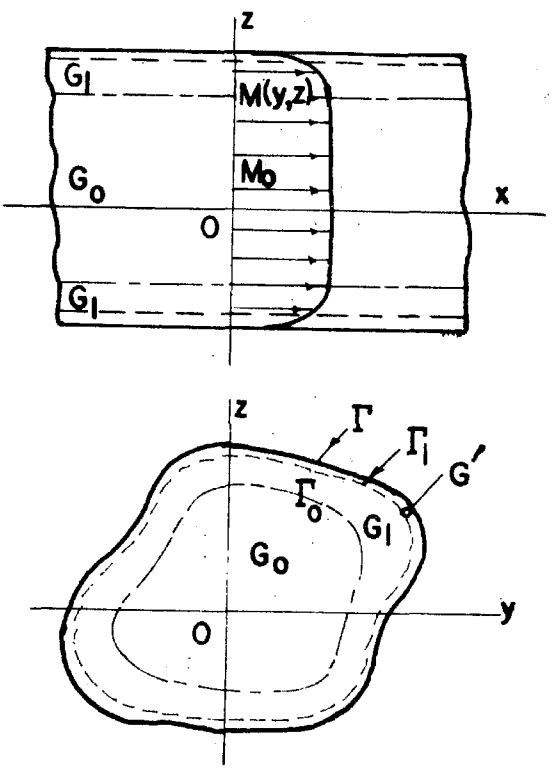

Fig. 1. The unperturbed flow.

$$U = M\sqrt{\gamma \frac{P}{R}} \qquad \gamma = c_p/c_v \tag{2.1}$$

where γ is the ratio of specific heats.

There is a central region G_0 within the cylindrical boundary Γ_0, where the Mach number has the constant value M_0 (see Figure 1). Since transonic flow fields are the subjects of this study, M_0 will be close to

one. Outside G_o is the wall boundary layer[+], through which M continuously and monotonously decreases from M_o to $M = 0$ at the wall. The boundary layer profile should be stable to small perturbations. The viscous sublayer G' next to the wall, within which viscous stress is not negligible, may be thought of as defined by the condition $M/M_o < 1/3$ (see also the fourth footnote of the next section). The region between G_o and G' will be denoted by G_1 and its inner boundary by Γ_1. In what follows G_1 will be called simply the boundary layer. Thus, the perturbation field to be studied by means of non-viscous theory occupies the region $G_o + G_1$ within the boundary Γ_1.

2.2 Perturbation equations

Let a slender model of finite upstream length be introduced in the central region G_o. It shall be assumed that no separation occurs, and that the velocity perturbation is everywhere steady and small compared to the undisturbed velocity, local exceptions being permitted in the immediate neighborhood of the model and its wake (see also paragraph 2.4).

Denoting the velocity perturbations in the direction of the x- y- and z-axes by u,v and w respectively, and the perturbed values of the pressure and density by p and ρ, we have the following system of first order quasi-linear differential equations for the unknown functions u, v, w, ρ and p in $G_o + G_1$ (except at shock waves):

$$\left.\begin{aligned} D(U+u) + \frac{1}{\rho}\frac{\partial p}{\partial x} &= 0 \\ Dv + \frac{1}{\rho}\frac{\partial p}{\partial y} &= 0 \\ Dw + \frac{1}{\rho}\frac{\partial p}{\partial z} &= 0 \end{aligned}\right\} \qquad (2.2)$$

[+]We here consider the Mach number boundary layer, which, however, in practice is not much different from the velocity boundary layer.

$$\left.\begin{aligned} D\rho - \frac{1}{a^2} Dp = 0 \\ \rho\left(\frac{\partial u}{\partial x} + \frac{\partial v}{\partial y} + \frac{\partial w}{\partial z}\right) + D\rho = 0 \end{aligned}\right\} \qquad \text{(2.2 cont'd.)}$$

D stands for the differential operator

$$D \equiv (U+u)\frac{\partial}{\partial x} + v\frac{\partial}{\partial y} + w\frac{\partial}{\partial z}$$

and a is the local speed of sound:

$$a = \sqrt{\gamma \frac{p}{\rho}} \qquad (2.3)$$

The equations express the conservation of momentum, mass and entropy along a streamline[+].

It is well known that linearizing the system (2.2) does not provide a good approximation for those parts of the perturbation field where the flow is of transonic character. Physically this is closely connected with the fact that the mass flow density has a maximum at the speed of sound. Mathematically it shows up in the fact that the system (2.2) changes from elliptic[++] to hyperbolic type when the speed of sound is attained, a behavior which is reproduced by the approximate equations only if certain quadratic terms are kept.[+++]

With the system (2.2) there is associated a characteristic form $C(\xi)$ (see Reference 12, p. 141), which is of the fifth degree in three independent variables, ξ_1, ξ_2, and ξ_3 say. Using the notation

$$D(\xi) \equiv (U+u)\xi_1 + v\xi_2 + w\xi_3$$

+ The entropy change through a weak shock wave is negligible in the approximation to be presently used.

++ We here call the equations elliptic if they have no other characteristic curves than the stream lines.

+++ It might be argued that linearization is not permitted where M/M_0 is small, since the velocity perturbation may be large compared to U. However, by definition we have $M/M_0 \geq 1/3$ in $G_0 + G_1$.

we have

$$C(\xi) \equiv \begin{vmatrix} u & v & w & \varrho & p \\ D(\xi) & 0 & 0 & 0 & \frac{1}{\rho}\xi_1 \\ 0 & D(\xi) & 0 & 0 & \frac{1}{\rho}\xi_2 \\ 0 & 0 & D(\xi) & 0 & \frac{1}{\rho}\xi_3 \\ 0 & 0 & 0 & D(\xi) & -\frac{1}{a^2}D(\xi) \\ \rho\xi_1 & \rho\xi_2 & \rho\xi_3 & D(\xi) & 0 \end{vmatrix} = D^3(\xi)\left[\frac{1}{a^2}D^2(\xi) - \xi_1^2 - \xi_2^2 - \xi_3^2\right] \qquad (2.4)$$

The circumscribed symbols indicate how the determinant has been formed from the coefficients of the derivatives of u, v, w, ϱ, and p. If $C/D^3(\xi)$ is a definite form, then the system (2.2) is elliptic. The necessary condition is seen to be $(U+u)^2 + v^2 + w^2 < a^2$, i.e. subsonic speed.

We now form a system of approximate equations from the equations (2.2) by dropping or adding in the coefficients terms which are of first of higher degree with respect to the non-dimensional perturbations $\frac{u}{U}, \frac{v}{U}, \frac{w}{U}, \frac{\rho-R}{R}$, and $\frac{\varrho-P}{P}$. The approximate system has a new characteristic form $C'(\xi)$ giving a condition for the system to be elliptic. This condition requires an approximate value for local Mach number to be less than one. If only zero order terms are kept in the coefficients - giving linear equations - the condition is $U < A$, and the approximate equations connot represent a field of mixed character. We then have to look for the simplest system for which C' gives a one step better approximation to the local Mach number, namely[+]

$$\frac{(U+u)^2+v^2+w^2}{a^2} \simeq M^2\left(1+2\frac{u}{U}+\frac{\rho-R}{R}-\frac{p-P}{P}\right) \qquad (2.5)$$

Inspecting the determinant in equation 2.4 one realizes that it is sufficient to keep a first order perturbation in the position (4) (p), and we make this

---

[+]In deriving this expression it has been assumed that $(\frac{v}{U})^2$ and $(\frac{w}{U})^2$ are negligible compared to $\frac{u}{U}$, $\frac{\rho-R}{R}$, and $\frac{p-P}{P}$. The assumption seems reasonable for the greater part of the field, but local exceptions may exist, for example close to a body of revolution (see Reference 13) or free vortices.

our choice. There are other possibilities which are equally simple, but they are all equivalent with the one chosen. The resulting system is

$$\left.\begin{aligned} &U\frac{\partial u}{\partial x}+\frac{1}{R}\frac{\partial p}{\partial x}+U_y v+U_z w=0\\ &U\frac{\partial v}{\partial x}+\frac{1}{R}\frac{\partial p}{\partial y}=0\\ &U\frac{\partial w}{\partial x}+\frac{1}{R}\frac{\partial p}{\partial z}=0\\ &U\frac{\partial p}{\partial x}-\frac{M^2}{U}\left(1+2\frac{u}{U}-\frac{\rho-R}{R}-\frac{p-P}{P}\right)\frac{\partial p}{\partial x}=0\\ &R\left(\frac{\partial u}{\partial x}+\frac{\partial v}{\partial y}+\frac{\partial w}{\partial z}\right)+U\frac{\partial p}{\partial x}=0 \end{aligned}\right\} \qquad (2.6)$$

It has the characteristic form

$$C'(\xi)=U^3\xi_1^3\left[M^2\left(1+2\frac{u}{U}+\frac{\rho-R}{R}-\frac{p-P}{P}\right)\xi_1^2-\xi_1^2-\xi_2^2-\xi_3^2\right]$$

showing that the system 2.6 is elliptic for $M^2\left(1+2\frac{u}{U}+\frac{\rho-R}{R}-\frac{p-P}{P}\right)<1$ as required by the condition (2.5).

2.3 The perturbation potential

To simplify the equations (2.6) we introduce a perturbation potential $\varphi(x,y,z)$ such that

$$\frac{\partial\varphi}{\partial x}=-\frac{1}{M_0^2}\frac{p-P}{\gamma P};\quad \frac{\partial\varphi}{\partial y}=\frac{M^2(Y,Z)}{M_0^2}\frac{v}{U(Y,Z)};\quad \frac{\partial\varphi}{\partial z}=\frac{M^2(Y,Z)}{M_0^2}\frac{w}{U(Y,Z)} \qquad (2.7)$$

thereby satisfying identically the second and third of the equations. (For U and M constant φ reduces to the usual velocity potential.) By elimination of $\frac{\partial\rho}{\partial x}$ and $\frac{\partial u}{\partial x}$ the following equation for φ is obtained+:

$$\left[1-M^2\left(1+2\frac{u}{U}+\frac{\rho-R}{R}-\frac{p-P}{P}\right)\right]\frac{\partial^2\varphi}{\partial x^2}+M^2\frac{\partial}{\partial y}\left(\frac{1}{M^2}\frac{\partial\varphi}{\partial y}\right)+M^2\frac{\partial}{\partial z}\left(\frac{1}{M^2}\frac{\partial\varphi}{\partial z}\right)=0$$

+In Reference 14 Lighthill showed for the linear case in two dimensions that the pressure perturbation satisfies a comparatively simple equation where M appears but not U or R separately. The "pressure potential" φ introduced above was inspired by this fact.

To express the coefficient of φ_{xx} by φ further approximations are necessary. Along a steamline we have

$$\frac{\rho(X,Y,Z)}{R(Y,Z)} = \left[\frac{p(X,Y,Z)}{P}\right]^{1/\gamma};$$

$$\frac{u(X,Y,Z)}{U(Y,Z)} + \frac{u^2+v^2+w^2}{2U^2(Y,Z)} + \frac{\gamma}{(\gamma-1)U^2}\left[\frac{p(X,Y,Z)}{\rho(X,Y,Z)} - \frac{P}{R(Y,Z)}\right] = 0$$

where Y,Z are the streamline coordinates far upstream. In a linear approximation this gives

$$\left.\begin{aligned} &\frac{\rho-R(Y,Z)}{R} = \frac{1}{\gamma}\,\frac{p-P}{P} + \frac{Grad\,R}{R}\cdot(\Delta Y,\Delta Z) \\ &(\Delta Y,\Delta Z) = \frac{M_0^2}{M^2}\int_{-\infty}^{X} Grad\,\varphi(\xi,Y,Z)\,d\xi \\ &\frac{u}{U} = -\frac{1}{\gamma M^2}\,\frac{p-P}{P} = \frac{M_0^2}{M^2}\,\frac{\partial\varphi}{\partial X} \end{aligned}\right\} \qquad (2.8)$$

The differential operator Grad is, for a given value of x, defined with respect to the y- and z- axes as the symbolic vector $\left(\frac{\partial}{\partial Y}, \frac{\partial}{\partial Z}\right)$. The vector $(\Delta y, \Delta z)$ has as components the streamline perturbations $\Delta y = y - Y$ and $\Delta z = z - Z$ in the y- and z-direction respectively for a given value of x.

For the local Mach number we then have in the same approximation

$$M^2\left(1+2\frac{u}{U}-\frac{\rho-R}{R}+\frac{p-P}{P}\right) = M^2 + M_0^2(\gamma+1)\left[1-\frac{\gamma-1}{\gamma+1}(1-M^2)\right]\frac{\partial\varphi}{\partial X} + M^2\,\frac{Grad\,R}{R}\cdot(\Delta Y,\Delta Z) \qquad (2.9)$$

where the perturbation terms are of essential importance only where $M \simeq 1$, i.e. in G_0 and the neighboring part of G_1. But here $\frac{Grad\,R}{R}\cdot(\Delta y, \Delta z)$ is very small under the reasonable assumption that the stagnation temperature does not vary much between the streamlines[+]. We shall therefore neglect the

---

[+]Since $\frac{GRAD\,R}{R} \simeq \frac{\gamma-1}{\gamma+1}\,GRAD\,M^2 = \frac{1}{6}\,GRAD\,M^2$ (for air with $\gamma = 1.4$).

term of equation (2.9) and put the factor $1-\frac{\gamma-1}{\gamma+1}(1-M^2)$ of the second term equal to one. As an additional argument may be used the fact that the vectors Grad R and $(\Delta y, \Delta z)$ are essentially orthogonal in the neighborhood of the wall, where the two vectors are not necessarily small.+

The differential equation for φ in the region $G_o + G_1$ (with shock waves excluded) finally takes the form

$$\left[1-M^2(Y,Z)\right]\frac{\partial^2\varphi}{\partial x^2}+M^2\frac{\partial}{\partial Y}\left(\frac{1}{M^2}\frac{\partial\varphi}{\partial Y}\right)+M^2\frac{\partial}{\partial Z}\left(\frac{1}{M^2}\frac{\partial\varphi}{\partial Z}\right)=M_o^2(\gamma+1)\frac{\partial\varphi}{\partial X}\frac{\partial^2\varphi}{\partial X^2} \qquad (2.10)$$

It is seen to be a straightforward generalization of the well known transonic equation when the undisturbed flow is uniform.

2.4 Boundary conditions

The perturbation potential has to satisfy boundary conditions at the model and its wake, at the shock waves, far upstream and downstream, and finally at the wall boundary Γ_1 (see Figure 1).

The theory to be developed aims at studying the wall interference under such conditions for which the flow in the immediate neighborhood of the model can be interpreted as belonging to some unbounded flow field.++ We will have to introduce this requirement by applying approximate boundary conditions at the boundary of this neighboring region, and therefore we can leave out a detailed analysis of the boundary conditions at the model and its associated shock and wake system.+++ The approximate boundary conditions will be discussed later.

+ In the free jet case, which will be treated subsequently, φ_{xx} is negligible at Γ_1, and the non-linear term of the differential equation can be neglected altogether.

++ This is the condition for a model test to be significant.

+++ For the same reason we permitted locally strong perturbations within the region mentioned in deriving the perturbation equations.

The shock polar in a proper approximation furnishes a condition for the velocity jump through a shock wave. Denoting the velocity vectors in front of and behind the shock respectively by $\mathbb{V}_1$ and $\mathbb{V}_2$ the shock polar has the following equation.

$$\mathbb{V}_1^2\mathbb{V}_2^2-(\mathbb{V}_1\cdot\mathbb{V}_2)^2=(\mathbb{V}_1^2-\mathbb{V}_1\mathbb{V}_2)^2\frac{\mathbb{V}_1\cdot\mathbb{V}_2-a_*^2}{\frac{2}{\gamma+1}\mathbb{V}_1^2-\mathbb{V}_1\cdot\mathbb{V}_2+a_*^2} \tag{2.11}$$

where a_* is the critical speed defined by

$$a_*^2(Y,Z)=\gamma\frac{p}{R(Y,Z)}\left[1-\frac{\gamma-1}{\gamma+1}(1-M^2(Y,Z))\right]$$

Introduction of the perturbation potential φ by equations (2.7) and of the approximations of equations (2.8) lead to the following approximate shock polar (see References 15 and 16)

$$(1-M_\infty^2)(\varphi_{x2}-\varphi_{x1})^2+(\varphi_{y2}-\varphi_{y1})^2+(\varphi_{z_2}-\varphi_{z_1})^2=M_\infty^2(\gamma+1)\frac{\varphi_{x1}+\varphi_{x2}}{2}(\varphi_{x2}-\varphi_{x1})^2 \tag{2.12}$$

where $\varphi_{x2}-\varphi_{x1}$ is the jump of $\frac{\partial\varphi}{\partial x}$ etc.

Since the upstream length of the model is finite the upstream condition is $\varphi_x=\varphi_y=\varphi_z=0$ for $x\longrightarrow-\infty$. The presence of a wake makes it difficult to give a simple downstream condition[+]. We will have to return to this problem later.

The boundary condition at the wall boundary Γ_1 is taken to be

$$(x,y,z)\longrightarrow\Gamma_1\ ;\ \frac{\partial\varphi}{\partial n}=0 \tag{2.13}$$

where $\frac{\partial}{\partial n}$ is the derivative along the inward normal. In the laminar case viscous effects within the sublayer G' might be taken into account by prescribing $\frac{\partial\varphi}{\partial n}$ as a suitable linear functional of φ on Γ_1 (see References 6 and 7)[++].

[+] In addition the assumption of an essentially nonviscous perturbation mechanism for the wall boundary layer is not a realistic one far downstream.

[++] The laminar sublayer is too thin to permit the use of the same approach to a turbulent boundary layer, although this was possible in shock wave interaction case (see Reference 6), where the length of the perturbed region is very small. An extension to include the perturbation of the turbulent stress seems difficult.

If the test section is not bounded by a wall but is a free jet, then the boundary condition at Γ_1 can be taken to be

$$(x,y,z) \to \Gamma_1 \quad : \quad \varphi = 0 \tag{2.14}$$

The condition is still applicable if only part of the boundary is free; this part must, however, be cylindrical to permit M to be independent of x.

It is by no means certain that the differential equation (2.10) together with the boundary conditions discussed defines a mathematically correct boundary value problem for the perturbation potential φ, although this seems to be the case if the flow is everywhere subsonic. Since the problem is non-linear, there is no general analytic method of solution. We therefore will have to restrict the present theory to serve as a starting point for further simplifications, and as a tool for phenomenological study.

2.5 Approximations for thin boundary layers

When the boundary layer at a wall is sufficiently thin compared to some characteristic length for the pressure perturbation then - as is known from boundary layer theory - the pressure is essentially constant through the boundary layer G_1[+]. This fact can be used to integrate the perturbation equation in G_1 approximately. In the free jet case it is rather the streamline slope that should be taken constant to make possible an approximate integration.

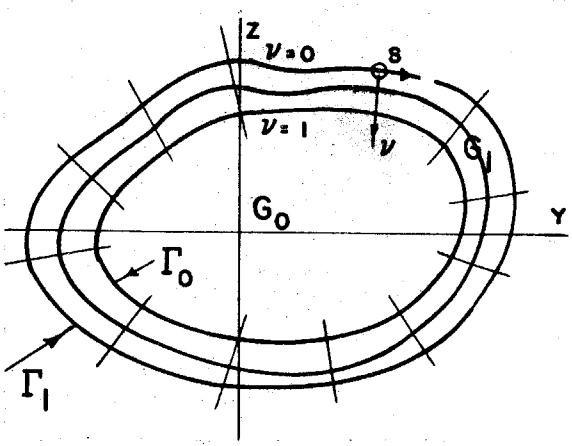

Fig. 2. Orthogonal coordinates for the boundary layer.

Let us introduce new orthogonal coordinates x, ν, s within the boundary

---

[+]The situation then is somewhat controversial since we have earlier assumed the length of the perturbed part of the boundary layer to be short. It will be seen later that there is enough room left for the present approximation to be applicable.

layer G_1, surfaces ν = constant being the cylinders of constant Mach number M, and s being the arc length along Γ_1 in a plane x = constant (see Figure 2). For simplicity we assume the form of the Mach number profile to be the same in all surfaces s = constant, although the boundary layer thickness δ may be a function of s. Not only Γ_0 but also Γ_1 are then surfaces ν = constant; we chose $\nu = 0$ for Γ_1 and $\nu = 1$ for Γ_0. We furthermore assume δ to be smaller than the local radius of curvature of Γ_1, in fact small enough to make the following metric form valid

$$dX^2 + dY^2 + dZ^2 \equiv dX^2 + \delta^2(s)\,d\nu^2 + \left[1 - \nu\delta\kappa(s)\right]^2 ds^2 \qquad (2.15)$$

Since evidently κ is the curvature of Γ_1 we have $\left[\delta(s)\,\kappa(s)\right] < 1$. If Γ_0 and Γ are concentric circles the form (2.15) is exactly valid.

With the new coordinates the differential equation (2.10) for φ takes the following form in G_1 (i.e. for $0 < \nu < 1$)

$$\frac{\partial}{\partial X}\left[\delta(1-\nu\delta\kappa)\,\frac{1-m^2M_0^2-M_0^2\frac{\gamma+1}{2}\frac{\partial\phi}{\partial X}}{m^2}\,\frac{\partial\phi}{\partial X}\right] + \frac{\partial}{\partial\nu}\left[\frac{1-\nu\delta\kappa}{\delta}\,\frac{1}{m^2}\,\frac{\partial\phi}{\partial\nu}\right] +$$

$$+ \frac{\partial}{\partial s}\left[\frac{\delta}{1-\nu\delta\kappa}\,\frac{1}{m^2}\,\frac{\partial\phi}{\partial s}\right] = 0 \qquad (2.16)$$

where

$$\phi(X,\nu,s) \equiv \varphi\left[X, Y(\nu,s), Z(\nu,s)\right], \quad m(\nu) \equiv \frac{1}{M_0}M\left[Y(\nu,s), Z(\nu,s)\right] \qquad (2.17)$$

When ϕ, and hence ϕ_x and ϕ_s, do not depend upon ν, equation (2.16) can be integrated with respect to ν. Using the boundary condition (2.13) at Γ_1 one obtains a value for $\frac{\partial\phi}{\partial n}$ $\left(= \frac{1}{\delta}\frac{\partial\phi}{\partial\nu}\right)$ on Γ_0 which is $0(\delta)$. Hence one concludes that

$$\phi(X,1,s) - \phi(X,0,s) = o(\delta^2)$$

and thus the hypothesis of constant pressure for δ small is seen to be consistent.

The expression for $\frac{\partial \phi}{\partial n}$ on Γ_o could be used as a new boundary condition for ϕ in G_o. It would however be unnecessarily complicated, being non-linear and applying at a changing boundary. We will therefore derive a condition on Γ_1 by continuing ϕ from G_o through the boundary layer according to the differential equation valid in G_o[+]:

$$(1-M_o^2)\frac{\partial^2\phi}{\partial X^2} + \frac{\partial^2\phi}{\partial Y^2} + \frac{\partial^2\phi}{\partial Z^2} = M_o^2(\gamma+1)\frac{\partial\phi}{\partial X}\frac{\partial^2\phi}{\partial X^2} \qquad (2.18)$$

We thus substitute for $\phi(x,\nu,s)$ in G_1 a new function $\bar{\phi}(x,\nu,s)$ satisfying the differential equation

$$\frac{\partial}{\partial X}\left[\delta(1-\nu\delta\kappa)\left(1-M_o^2-M_o^2\frac{\gamma+1}{2}\frac{\partial\bar{\phi}}{\partial X}\right)\frac{\partial\bar{\phi}}{\partial X}\right] + \frac{\partial}{\partial\nu}\left[\frac{1-\nu\delta\kappa}{\delta}\frac{\partial\bar{\phi}}{\partial\nu}\right] + \frac{\partial}{\partial s}\left[\frac{\delta}{1-\nu\delta\kappa}\frac{\partial\bar{\phi}}{\partial s}\right] = 0 \qquad (2.19)$$

(obtained from (2.16) for m = 1) and the boundary conditions

$$\nu = 1: \quad \bar{\phi} = \phi, \quad \frac{\partial\bar{\phi}}{\partial n} = \frac{\partial\phi}{\partial n} \qquad (2.20)$$

in some consistent approximation. If the difference is taken between equations (2.16) and (2.19) one obtains the expression

$$\frac{\partial}{\partial X}\left\{\delta(1-\nu\delta\kappa)\left[\frac{1-m^2}{m^2}\left(1-M_o^2\frac{\gamma+1}{2}\frac{\partial\bar{\phi}}{\partial X}\right)\frac{\partial\bar{\phi}}{\partial X} + \frac{1-m^2M_o^2-M_o^2\frac{\gamma+1}{2}(\phi_X+\bar{\phi}_X)}{m^2}\frac{\partial}{\partial X}(\phi-\bar{\phi})\right]\right\} +$$

$$\frac{\partial}{\partial\nu}\left[\frac{1-\nu\delta\kappa}{\delta}\left(\frac{1}{m^2}\frac{\partial\phi}{\partial\nu} - \frac{\partial\bar{\phi}}{\partial\nu}\right)\right] + \frac{\partial}{\partial s}\left\{\frac{\delta}{1-\nu\delta\kappa}\left[\frac{1-m^2}{m^2}\frac{\partial\bar{\phi}}{\partial s} + \frac{1}{m^2}\frac{\partial}{\partial s}(\phi-\bar{\phi})\right]\right\} = 0 \qquad (2.21)$$

which we will integrate with respect to ν under the conjecture that

$$\bar{\phi}(X,\nu,s) - \phi(X,\nu,\delta) = O(\delta^2)$$

[+]The conditions for the continuation to be possible are essentially the same as these permitting the present approximation for thin boundary layers.

Since the variation of ϕ through the boundary layer is $O(\delta^2)$ the same has to be true for $\bar{\phi}$, and equation (2.21) simplifies to

$$\frac{\partial}{\partial \nu}\left[\frac{1-\nu\delta K}{\delta}\left(\frac{\partial \bar{\phi}}{\partial \nu}-\frac{1}{m^2}\frac{\partial \phi}{\partial \nu}\right)\right]=\frac{\partial}{\partial X}\left[\delta(1-\nu\delta K)\frac{1-m^2}{m^2}\bar{\phi}_X(X,0,S)\right]+$$

$$+\frac{\partial}{\partial S}\left[\delta(1+\nu\delta K)\frac{1-m^2}{m^2}\bar{\phi}_S(X,0,S)\right]+O(\delta^3) \qquad (2.22)$$

As a further approximation the term $M_o^2\frac{\gamma+1}{2}\bar{\phi}_X$ here has been neglected against unity. Using the boundary conditions (2.13) and (2.20) the integration gives

$$\nu=0: \quad \frac{\partial \bar{\phi}}{\partial n}=-\varepsilon_1\delta\left(\frac{\delta^2}{\partial X^2}+\frac{\partial^2}{\partial S^2}+\frac{\delta'}{\delta}\frac{\partial}{\partial S}\right)\bar{\phi}+\frac{1}{2}\varepsilon_2 K\delta^2\left(\frac{\partial^2}{\partial X^2}-\frac{\partial^2}{\partial S^2}-\frac{1}{K\delta^2}\frac{dK\delta^2}{dS}\frac{\partial}{\partial S}\right)\bar{\phi}+$$

$$+O(\delta^3) \qquad (2.23)$$

where

$$\varepsilon_1=\int_o^1\frac{1-m^2}{m^2}d\nu, \quad \varepsilon_2=\int_o^1\frac{1-m^2}{m^2}d(\nu^2) \qquad (2.24)$$

The result is seen to be consistent with the initial conjecture. We therefore propose to use (2.23) as a boundary condition for φ on Γ_1 with the translation from $\bar{\phi}$ to φ as defined in equation (2.17), taking φ to satisfy the differential equation (2.18) not only in G_o but in G_1 as well[+].

The parameters ε_1 and ε_2, describing the form of the Mach number distribution of the unperturbed boundary layer, are defined only if $m = o(\nu)$ for $\nu \to o$. This of course is closely related to the fact that the viscous stress is more important than the mass forces at the wall. In restricting ourselves to turbulent boundary layers we assumed $m(o)$ to be greater than zero (we even proposed the value $m(o) = 1/3$) and thus ε_1 and ε_2 exist

---

[+]This boundary condition is not convenient for supersonic outer flow (see e.g. Reference 33). A modified condition is proposed in Appendix C.

in the present case. Taking $m = \nu^{1/6}$ as a typical profile[+] the following values are obtained

$$\varepsilon_1 = \tfrac{1}{2}\,(0.484) \qquad \varepsilon_2 = \tfrac{1}{5}\,(0.199) \tag{2.25}$$

The corresponding values when the integration is started at $m(\nu) = 1/3$ are given within parentheses. The contribution from the innermost part of the profile $m = \nu^{1/6}$ evidently is very small, and this fact supports the assumption that perturbation of the viscous sublayer does not contribute much to the displacement effect.

Turning to the case of a free jet we introduce in the same way an approximate continuation $\bar{\phi}$ of ϕ into G_1 by equations (2.19) and (2.20). From the boundary condition (2.14) we guess that ϕ and $\bar{\phi}$ are $O(\delta)$. It then follows from equation (2.16) and (2.19) that

$$\left.\begin{aligned} \frac{\partial \phi}{\partial \nu} &= m^2\,\frac{1-\delta K}{1-\nu\delta K}\left[\frac{\partial \phi}{\partial \nu}\right]_{\nu=1} + O(\delta^3) \\ \frac{\partial \bar{\phi}}{\partial \nu} &= \frac{1-\delta K}{1-\nu\delta K}\left[\frac{\partial \bar{\phi}}{\partial \nu}\right]_{\nu=1} + O(\delta^3) \end{aligned}\right\} \tag{2.26}$$

Integrating once more with respect to ν and introducing the boundary conditions (2.14) and (2.20), one obtains after some manipulations

$$\nu = \bar{\nu} = e_1 + \tfrac{1}{2}K\delta(e_2 - e_1^2) \;:\qquad \bar{\phi} = O(\delta^3) \tag{2.27}$$

where

$$e_1 = \int_0^1 (1-m^2)\,d\nu \quad , \quad e_2 = \int_0^1 (1-m^2)\,d(\nu^2) \tag{2.28}$$

This, then, is the approximate boundary condition to be applied at $\nu = \bar{\nu}$ to the continued perturbation potential φ. It is noteworthy that the new

---

[+] A natural turbulent boundary layer is considered. For artificially produced boundary layers ε_1 and ε_2 seem to be able to take values much different from those of (2.25).

boundary condition is of the same form as the original one, only it is to be applied at a slightly perturbed boundary (since $o < \bar{\nu} < 1$) which is uniquely determined by the boundary layer profile $m(\nu)$. Consequently the influence of the boundary layer on the boundary interference connot be great in the case of a free jet+.

The approximate boundary conditions derived are not valid in the neighborhood of sharp corners of the test section. It does not seem too difficult, however, to estimate the errors which are introduced by applying them there. If the test section is partly closed, partly open similar errors are bound to occur in the neighborhood of the edges. One should for example not apply the approximate boundary conditions at a wall which is open along streamwise slots, unless their width and mutual distance are much larger than the boundary layer thickness.

2.6 Transonic similarity

For a thin boundary layer the perturbation problem has been reduced to that of finding a solution φ which in $G_o + G_1$ satisfies the classical transonic equation (2.18) and on the boundary Γ_1 satisfies the boundary condition (2.23) or (2.27). It is well known how a group property of solutions to the transonic equation can be used as the basis for deriving similarity rules for transonic flow fields. An application to wind tunnel flow is found in Reference 17.

Let $\varphi(x,y,z)$ be a solution, and transform to new coordinates ξ, η, ζ by putting

$$X = \xi \quad , \quad Y = \frac{\eta}{\beta} \quad , \quad Z = \frac{\zeta}{\beta} \quad , \quad \varphi(X,Y,Z) = \frac{\beta^2}{M_0^2(\gamma+1)} \psi(\xi,\eta,\zeta) \qquad (2.29)$$

+This is not surprising since the zero pressure perturbation at Γ_1 forces the mass flow density to stay essentially constant within the boundary layer - in contrast to the wall case.

where β is an arbitrary parameter if $M_o = 1$ and $\beta = \sqrt{|1-M_o^2|}$ if $M_o \neq 1$. The new function $\psi(\xi, \eta, \zeta)$ satisfies a differential equation which contains no other parameter than sign $(1-M_o)$. The same is true for the transformed shock polar of equation (2.12) (see Reference 15). A solution ψ for a given set of boundary conditions in the ξ, η, ζ-space then according to equation (2.29) generates in the physical space a group of solutions ϕ with the two parameters β and γ. If the transformed boundary conditions correspond to physically reasonable solutions ψ, we will say that the generated flow fields are similar.

To extend the similarity concept we evidently have to find out if the form of the boundary conditions is invariant under the transformation (2.29). In the wall case (equation 2.23) a necessary condition is seen to be that one can neglect the crossflow terms (i.e. terms containing derivatives with respect to s) since $\frac{\partial}{\partial x}$ and $\frac{\partial}{\partial s}$ transform differently[+]. Then the generated group of fields are similar if they have the same value for $\frac{1}{\beta}\varepsilon, \delta$ and $\varepsilon_2\delta^2$ (the curvature κ transforms like $\frac{\partial}{\partial n}$). The most interesting case occurs if the δ^2-terms can be neglected, since then there exist similar fields with a fixed boundary layer profile $m(\nu)$.

The free jet case is simpler in several respects. There are no crossflow terms in the boundary condition (2.27). Similar fields are seen to have the same values for $e_1\beta\delta$ and $e_2\beta^2\delta^2$, and thus similarity permits preservation of $m(\nu)$ and of boundary layer thickness relative to test section size.

2.7 The linearized equations

There are transonic wall interference problems for which the dif-

---

[+]It should be noted that the streamwise terms express the essential part of the change of mass flow density in the boundary layer, since cross flow leaves unchanged the average mass flow density in a given cross section.

ferential equation (2.10) can be linearized (see next chapter). If in addition the boundary layers are thin enough for the approximate boundary conditions to be valid, then one has (after a Prandtl-Glauert transformation) a problem for either the Laplace equation ($M_o < 1$) or the wave equation ($M_o > 1$). In any case there are available powerful methods of solution - analytical as well as numerical. Since the boundary conditions are somewhat unusual there might be some question as to existence and uniqueness of solutions. In the subsonic analysis of Chapter III existence will be proved by actually constructing the solutions wanted. Two relevant uniqueness theorems for the subsonic case are given in Appendix B. A discussion of the supersonic case is given in Appendix C.

When the approximate boundary conditions cannot be applied one will have to solve the complete equation

$$(1-M^2)\frac{\partial^2\varphi}{\partial x^2} + M^2\frac{\partial}{\partial y}\left(\frac{1}{M^2}\frac{\partial\varphi}{\partial y}\right) + M^2\frac{\partial}{\partial z}\left(\frac{1}{M^2}\frac{\partial\varphi}{\partial z}\right) = 0 \qquad (2.30)$$

where M is a function of y and z. Only for simple functions M and for simple boundaries Γ_o and Γ_1 will analytical methods of solutions be useful. In many cases it will be convenient to express the solution as a Fourier integral with respect to x, and this might be true even when numerical or similar methods are used. As an example we will sketch an application of an electric analogy due to G.I. Taylor (Reference 19).

Taking $M_o < 1$, let the Fourier transform of φ in the x-direction exist and be $F(k;y,z)$, where k is the wave number. The transformed equation for F is:

$$\frac{\partial}{\partial y}\left(\frac{1}{M^2}\frac{\partial F}{\partial y}\right) + \frac{\partial}{\partial z}\left(\frac{1}{M^2}\frac{\partial F}{\partial z}\right) = \frac{1-M^2}{M^2}K^2F \qquad (2.31)$$

which for $-\infty < K < \infty$ has to be solved within the projection of Γ_1 on

the y z-plane. It shall be assumed that we know particular solutions g(k; y,z) which are everywhere positive in the region under consideration[+]. Writing F in the form F = g . G (k; y,z), the new unknown function G has to satisfy the differential equation

$$\frac{\partial}{\partial Y}\left(\frac{g^2}{M^2}\frac{\partial G}{\partial Y}\right)+\frac{\partial}{\partial Z}\left(\frac{g^2}{M^2}\frac{\partial G}{\partial Z}\right)=0 \qquad (2.32)$$

which is of the form required by the analogy.

The analogue to be considered is the approximately plane electric field in a thin conducting layer spread over the y z-plane. The thickness of the layer is a function of y and z, and it shall be determined in such a way that either the continuity equation or the condition of irrotationality of the current field is of the same form as equation (2.32). In the first case G is taken proportional to the electric potential (or rather the mean value of the potential through the layer), and the proper thickness of the layer is found to be proportional to $\left[g(k;\, y,z)/M(y,z)\right]^2$. In the second case G is taken to be proportional to the stream function, leading to a thickness distribution which is inversely proportional to $(g/M)^2$.

In practice the analogue is realized as a thin layer of conducting fluid between a free surface and a properly shaped bottom of insulating material. The boundary conditions are introduced by controlling the potential and current of properly arranged electrodes at the boundaries. In each specific application solutions G have to be determined for a series of values for k. Since the thickness distribution depends upon k, this means that a series of different bottoms will have to be used.

[+]Since the solutions are not required to be analytically given, nor to satisfy any specific boundary conditions, the problem of determining them is likely to be simpler than the original one.

III. LINEAR CORRECTIONS

3.1 Introduction

To a limited extent linear theory may be used for computing the wall interference at transonic tests. An essential condition would be that the flow is of transonic character only around the model in a limited region, the lateral extension of which is small compared to its distance from the walls. When linear corrections can be determined, they often - but not always - are so small that the influence of the wall boundary layers may be neglected (Problem I of paragraph 1.3). This tends of course to limit the practical importance of a linear theory for the boundary layer influence. On the other hand, artificial thickening of the boundary layers might permit linear corrections to be used at higher Mach numbers where the contribution of the wall boundary layers is not negligible (Problem II).

The linear theory permits solutions at the lower limit of a Mach number range where boundary layer effects are likely to be large, and where there are no solutions to hope for. It seems possible to discuss boundary layer effects also at the upper limit - i.e. at choking - in comparatively simple terms (see Chapter IV). The results of linear theory may therefore be important as a tool for interpolation in the Mach number range mentioned. This point as well as other points related to Problems I and II will be more closely examined in the concluding chapter.

The simple cases of plane and circular closed test sections with centrally located models will be treated, accounting for the wall boundary layers by means of the approximate boundary condition of paragraph 2.5.

The linear method for computing wall corrections is well developed for practical use in the case of negligible boundary layer influence. For a survey the reader is referred to References 1 and 2.

3.2 The correction procedure

In correcting wind tunnel tests for wall interference one has to introduce the basic hypothesis that in some neighborhood of the model the flow agrees sufficiently well with the corresponding part of the unbounded flow field about the same model for some values of free-stream Mach number and angle of attack.

One might imagine technically sensible wind tunnel flows to be set up in the following way. Starting with the unbounded flow field at free-stream Mach number $M_\infty < 1$ around the given model at angle of attack α_∞, one introduces an initially large test section which uniformly decreases in size (together with its boundary layers) towards a final configuration. During this process the model is fixed in space, and the relative position of the test section with respect to a point in the model is kept the same, while the Mach number M_0 far upstream and the angle α_0 between the wall generators and the model are successively adjusted to leave the field in the neighborhood of the model in some sense unchanged. As a criterion one can for example choose to keep the drag and the lift constat (for a given stagnation pressure). As long as the criterion is not violated the wall correction ΔM_0 and $\Delta\alpha_0$ can be defined by putting

$$M_\infty = M_0 + \Delta M_0 \quad , \quad \alpha_\infty = \alpha_0 + \Delta\alpha_0 \tag{3.1}$$

If the size of the test section is further decreased it finally reaches a smallest value consistent with the criterion for unchanged flow at the model. Test results from a smaller test section can not be interpreted as belonging to the given values of M_∞ and α_∞.

In a test section of the minimum size the region of unchanged flow at the model probably is small, but it is bound to increase with the size of

the test section. When the test section is sufficiently large, that part of the field where linear theory is not applicable will be situated completely within the region of unchanged flow. The linear theory then can be used for computing the wall interference.

Thus we have defined two lower bounds for the test section size: below the first one corrections do not exist, and below the second one the corrections cannot be computed by linear theory. The two bounds may be equal. Both of them increase strongly for M_∞ approaching one.

We now restrict ourselves to the case where the linear theory and the approximate boundary condition at the wall are applicable. Let $\varphi_o(x,y,z)$ be the perturbation potential for a given model at the angle of attack α_o in a test section with the upstream Mach number $M_o < 1$. Here x,y,z are Cartesian coordinates as defined in Figure 1. For simplicity the model and the test section are assumed to be symmetrical with respect to the plane $z = 0$. Let $\varphi_\infty(x,y,z)$ be the perturbation potential for the same model in unbounded flow with the corrected values M_∞ and α_∞ of free-stream Mach number and angle of attack respectively. We define φ_∞ like φ_o to describe the perturbation of a uniform flow of Mach number M_o parallel to the test section (see equation (2.7) and paragraph 2.5)[++]. A similarly defined perturbation potential $\varphi_w(x,y,z)$ for the wall interference is introduced by putting

$$\varphi_o = \varphi_\infty + \varphi_w \tag{3.2}$$

within the test section. The arbitrary additive constant is fixed to make $\varphi_w = 0$ at some representative point at the model.

[+] It is supposed to occupy a neighborhood of the model and the leading part of the wake. Further downstream in the wake linear theory may not be strictly applicable, but no errors should be introduced at the model by applying it.

[++] The errors introduced by not referring φ_∞ to the unbounded uniform flow are of second order, otherwise linear theory could not be used for computing ΔM_o and $\Delta\alpha_o$.

According to the initial assumptions φ_o and φ_∞ satisfy the linear differential equation

$$(1-M_o^2)\frac{\partial^2\varphi}{\partial X^2} + \frac{\partial^2\varphi}{\partial Y^2} + \frac{\partial^2\varphi}{\partial Z^2} = 0 \tag{3.3}$$

except in a neighborhood of the model and the leading part of the wake, where they are practically identical. Thus their difference φ_w can be taken to satisfy equation (3.3) everywhere in the test section $(G_o + G_1)$.

If φ_∞ is known in the neighborhood of the wall a boundary condition for φ_w at Γ_1 is obtained by introducing equation (3.2) into the boundary condition (2.23) for φ_o. Likewise the conditions $\varphi_{ox} - \varphi_{oy} = \varphi_{oz} = 0$ for $x \to -\infty$ give a set of upstream conditions for φ_w :

$$X \to -\infty : \quad \varphi_{wx} = -\frac{1}{1+\frac{\gamma-1}{2}M_o^2}\,\frac{\Delta M_o}{M_o}, \quad \varphi_{wy} = -\frac{M_\infty^2}{M_o^2}\Delta\alpha_o, \quad \varphi_{wz} = 0 \tag{3.4}$$

These are not necessarily valid for $x \to +\infty$, since there is a wake downstream. A sensible choice seems to be

$$X \to \infty : \quad \varphi_{wxx} = \varphi_{wyx} = \varphi_{wzx} = 0 \tag{3.5}$$

The boundary conditions thus specified should be sufficient for determining φ_w as a function of the corrections ΔM_o and $\Delta\alpha_o$. These two parameters consequently are the only ones at our disposal for fulfilling the condition of zero perturbation at the model. The simplest way of specifiying this condition is to require that

$$X = Y = Z = 0 \quad : \quad \varphi_{wx} = \varphi_{wy} = 0 \tag{3.6}$$

taking as origin a suitable point at the model (where $\varphi_w = 0$). By symmetry one automatically has $\varphi_{wz} = 0$.

After having determined ΔM_o and $\Delta\alpha_o$ from the conditions (3.6) one

will have to establish the applicability of the correction procedure by checking that φ_{wx}, φ_{wy} and φ_{wz} are sufficiently small in the transonic region around the model.

From the preceding analysis it is seen that the corrections can be computed if one knows φ_∞ and its normal derivative at the wall. When the flow at the model is not of transonic character φ_∞ can be computed by linear theory, but in the present case we will have to estimate it from the pressure distribution at the wall, which easily can be measured.

3.3 Plane flow

Let the field be independent of the z-coordinate, and take the planes $y = \pm 1$ to be the walls (see Figure 3), carrying identical boundary layers of thickness δ. The model is situated at the origin, which is that representative point where the wall interference vanishes.

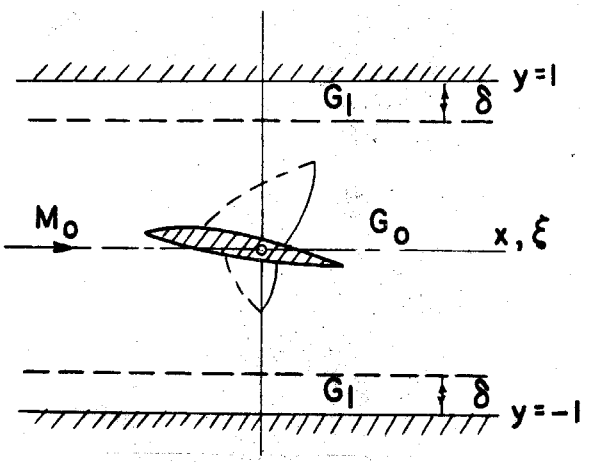

Fig. 3. Plane test section

The equations for the wall perturbation potential $\varphi_w(x,y)$ as derived in the preceding paragraph may be summarized in the following way:

$$
\left.
\begin{aligned}
&(1-M_0^2)\,\varphi_{wXX} + \varphi_{wYY} = 0 \quad \text{IN} \quad G_0 + G_1 \\
&X \to -\infty: \quad \varphi_{wX} = -\frac{1}{1+\frac{\gamma-1}{2}M_0^2}\,\frac{\Delta M_0}{M_0}\,, \quad \varphi_{wY} = -\frac{M_\infty^2}{M_0^2}\,\Delta\alpha_0 \\
&X \to \infty: \quad \varphi_{wXX} = 0\,, \quad \varphi_{wXY} = 0 \\
&Y = \pm 1: \quad \left(\frac{\partial}{\partial Y} \mp \varepsilon_1 \delta \frac{\partial^2}{\partial X^2}\right)(\varphi_w + \varphi_\infty) = 0 \\
&X = Y = 0: \quad \varphi_w = 0\,, \quad \varphi_{wX} = 0\,, \quad \varphi_{wY} = 0
\end{aligned}
\right\} \qquad (3.7)
$$

With no loss of generality the perturbation potential $\varphi_\infty(x,y)$ for unbounded flow may be taken to be given in the form

$$\varphi_\infty = \frac{\sqrt{1-M_\infty^2}}{1+\frac{\gamma-1}{2}M_0^2}\,\frac{\Delta M_0}{M_0}\,\xi + g^{00}(\xi,Y) + g^{10}(\xi,Y) +$$

$$+ \frac{M_\infty^2}{M_0^2}\,\Delta\alpha_0 Y + g^{01}(\xi,Y) + g^{11}(\xi,Y)\,; \quad \xi \equiv \frac{x}{\sqrt{1-M_0^2}} \tag{3.8}$$

where the functions g^{mn} are odd or even with respect to ξ for $m = 0$ and $m = 1$ respectively, and with respect to y for $n = 0$ and $n = 1$ respectively. They are harmonic functions outside a region where $y \ll 1$. The function g^{11} has a jump along the x-axis, but its derivatives are continuous there.

It is well know that for large values for $R^2 = \xi^2 + y^2$ the following estimates can be made:

$$\left.\begin{aligned} g^{00} &= O(\log R) \\ g^{10} &= O\left(\frac{\xi}{R^2}\right) \\ g^{01} &= O\left(\frac{Y}{R^2}\right) \\ g^{11} &= O\left(\tan^{-1}\frac{\xi}{Y}\right) \end{aligned}\right\} \tag{3.9}$$

For g^{11} the principal value of $\tan^{-1}$ is taken in the upper half plane. these asymptotic fields in order correspond to the following singularities at the origin : a source, a doublet in the ξ -direction, a doublet in the y-direction, and a vortex.

Similarly the wall perturbation potential shall be written in the following form

$$\varphi_W = -\frac{\sqrt{1-M_0^2}}{1+\frac{\gamma-1}{2}M_0^2}\,\frac{\Delta M_0}{M_0}\,\xi + h^{00}(\xi,Y) + h^{10}(\xi,Y) -$$

$$- \frac{M_\infty^2}{M_0^2}\,\Delta\alpha_0 Y + h^{01}(\xi,Y) + h^{11}(\xi,Y) \tag{3.10}$$

where the functions h^{mn} are harmonic for $|y| < 1$. Their properties of symmetry as indicated by the superscripts are similar to those of g^{mn}.

Introduction of the expressions (3.8) and (3.10) into the equations (3.7) gives a set of boundary value problems for h^{mn} in the half strip $0 \leq \xi < \infty$, $0 \leq y \leq 1$:

$$
\left.
\begin{aligned}
& h^{mn}_{\xi\xi} + h^{mn}_{YY} = 0 \\
& \xi \to \infty : \; h^{mo}_{\xi\xi} = 0, \; h^{oo}_{\xi} = h^{lo}_{\xi} = h^{mo}_{\xi Y} = 0; \; h^{m1}_{\xi} = 0 \\
& \xi = 0 : \; h^{on}_{\xi} = 0, \; h^{1n} = 0 \\
& Y = 1 : \; \left(\frac{\partial}{\partial Y} - \frac{\varepsilon_1 \delta}{1 - M_0^2} \frac{\partial^2}{\partial \xi^2}\right)(h^{mn} + g^{mn}) = 0 \\
& Y = 0 : \; h^{mo}_{Y} = 0, \; h^{m1} = 0
\end{aligned}
\right\} \quad m,n = 0 \text{ and } 1 \qquad (3.11)
$$

These equations would permit the functions h^{mn} to be determined separately, were it not for the connection between h^{oo} and h^{lo} in the condition for $\xi \to \infty$. The separation can however easily be completed. Since h^{oo} is harmonic in the half strip considered the line integral $\int \frac{\partial h^{oo}}{\partial n} ds$ taken around the closed path of Figure 4 is zero. This means, since $\frac{\partial h^{oo}}{\partial n} = 0$ on the coordinate axes, that

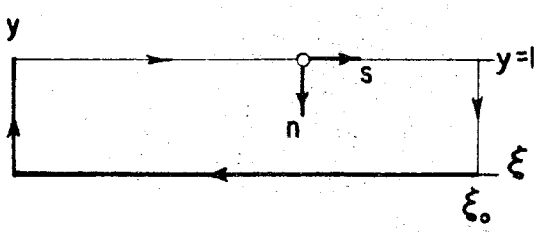

Fig. 4 Path of integration

$$\int_0^1 h^{oo}_{\xi}(\xi_0, Y)\, dY = -\int_0^{\xi_0} h^{oo}_{Y}(\xi, 1)\, d\xi$$

Using the boundary condition for $y = 1$, this can be written

$$\int_0^1 h^{oo}_{\xi}(\xi_0, Y)\, dY = \int_0^{\xi_0} g^{oo}_{Y}(\xi, 1)\, d\xi - \frac{\varepsilon_1 \delta}{1 - M_0^2}\left[h^{oo}_{\xi}(\xi_0, Y) + g^{oo}_{\xi}(\xi_0, Y)\right]$$

In the limit $\xi_0 \to \infty$ the result becomes

$$h^{oo}_{\xi}(\infty, Y) = h^{lo}_{\xi}(\infty, Y) = \frac{1}{1 + \frac{\varepsilon_1 \delta}{1 - M_0^2}} \int_0^{\infty} g^{oo}_{Y}(\xi, 1)\, d\xi = \frac{1}{2} \varphi_{0\xi}(\infty, 1) \qquad (3.12)$$

since $h^{00}_{y} = 0$ and $g^{00} = 0$ (log R) for $\xi \to \infty$. This completes the separation.

The condition of equation (3.7) for zero perturbation at the origin gives the following expressions for the correction ΔM_o and $\Delta \alpha_o$:

$$\Delta M_o = M_o \frac{1+\frac{\gamma-1}{2}M_o^2}{\sqrt{1-M_o^2}} h_\xi^{10}(0,0) \; ; \qquad \Delta \alpha_o = \frac{M_o^2}{M_\infty^2} h_Y^{01}(0,0) \tag{3.13}$$

which do not contain h^{00} or h^{11}. As a test of the correction procedure it might however be worth while to compute also the following quantities

$$\frac{D}{D\xi}\left[\Delta M_o\right] = M_o \frac{1+\frac{\gamma-1}{2}M_o^2}{\sqrt{1-M_o^2}} h_{\xi\xi}^{00}(0,0) \; ; \quad \frac{D}{D\xi}\left[\Delta \alpha_o\right] = \frac{M_o^2}{M_\infty^2} h_{\xi Y}^{11}(0,0) \tag{3.14}$$

the operator $\frac{D}{D\xi}$ denoting the rate of change due to a translation in ξ - direction of the representative point. One will have to require that those test quantities multiplied by some characteristic model length are much smaller than the corresponding correction.

To determine the functions h^{mn} as required by equations (3.13) and (3.14) we express the functions g^{mn} in the neighborhood of the walls by means of Fourier kernels $G^{mn}(k)$ in the following way:

$$\left.\begin{aligned}
g_{\xi\xi}^{00}(\xi,Y) &= \int_o^\infty G^{00}(K)\, e^{(1-|Y|)K} \cos \xi K \, dK \\
g_{\xi}^{10}(\xi,Y) &= \int_o^\infty G^{10}(K)\, e^{(1-|Y|)K} \cos \xi K \, dK \\
g^{01}(\xi,Y) &= \operatorname{sgn} Y \int_o^\infty G^{01}(K)\, e^{(1-|Y|)K} \cos \xi K \, dK \\
g_{\xi}^{11}(\xi,Y) &= \operatorname{sgn} Y \int_o^\infty G^{11}(K)\, e^{(1-|Y|)K} \cos \xi K \, dK
\end{aligned}\right\} \tag{3.15}$$

This is possible since g^{mn} are harmonic functions which for $\xi \to \infty$ behave according to the estimates (3.9). The kernels G^{mn} are continuous and exponentially decreasing for $k \to \infty$. For $k \to o$ we have $G^{mo} = O(|k|)$

since g^{00} and g^{10} are $O(\frac{1}{\xi})$ for $\xi \to \infty$.

Formally the solutions then are

$$\left.\begin{aligned} h_{\xi\xi}^{00} &= \int_0^\infty \frac{G^{00}(K)}{K} C(K) \cosh YK \cos \xi K \, dK \\ h_\xi^{10} &= \frac{1}{1+\frac{\varepsilon_1 \delta}{1-M_0^2}} \int_0^\infty g_Y^{00}(\xi,1)\, d\xi + \int_0^\infty \frac{G^{10}(K)}{K} C(K) \cosh YK \cos \xi K \, dK \\ h^{01} &= \int_0^\infty G^{01}(K) S(K) \frac{\sinh |Y_1| K}{K} \cos \xi K \, dK \\ h^{11} &= \int_0^\infty G^{11}(K) S(K) \frac{\sinh |Y_1| K}{K} \cos \xi K \, dK \end{aligned}\right\} \qquad (3.16)$$

where

$$\left.\begin{aligned} C(K) &\equiv K \frac{1-M_0^2-\varepsilon_1 \delta K}{(1-M_0^2)\sinh K + \varepsilon_1 \delta K \cosh K} \\ S(K) &\equiv K \frac{1-M_0^2-\varepsilon_1 \delta K}{(1-M_0^2)\cosh K + \varepsilon_1 \delta K \sinh K} \end{aligned}\right\} \quad K \geq 0 \qquad (3.17)$$

The functions C(k) and S(k) are continuous everywhere (since $\varepsilon_1 \delta \geq 0$ and $1-M_0^2 > 0$), and are $\sim k e^{-k}$ for $k \to \infty$. Hence there is no difficulty in showing that the solutions obtained satisfy the equations of the problem.

To conclude the analysis we have to express G^{mn} by the pressure distribution at the wall. We therefore put $\varphi_{0\xi}(\xi,1)$ in the form

$$\varphi_{0\xi}(\xi,1) = \sum_{m,n} f^{mn}(\xi), \qquad f^{mn}(\xi) \equiv g_\xi^{mn}(\xi,1) + h_\xi^{mn}(\xi,1) \qquad (3.18)$$

It follows from equations (3.15) and (3.16) that the functions f^{mn} can be expressed by means of Fourier kernels $F^{mn}(k)$ as follows:

$$f^{00}(\xi) = \frac{1}{2}\varphi_{0\xi}(\infty,1) \cdot \frac{\xi}{\sqrt{\xi^2+1}} + \int_0^\infty F^{00}(K) \sin \xi K \, dK \qquad (3.19)$$

$$f^{10}(\xi) = \frac{1}{2}\varphi_0\xi(\infty,1) + \int_0^\infty F^{10}(K)\cos\xi K\,dK$$

$$f^{01}(\xi) = \int_0^\infty F^{01}(K)\sin\xi K\,dK$$

$$f^{11}(\xi) = \int_0^\infty F^{11}(K)\cos\xi K\,dK$$

(3.19) cont'd.

After inverting the Fourier integrals the kernels F^{mn} are obtained as Fourier transforms of functions which can be experimentally determined[+]. Finally the following formulae for G^{mn} are derived by combining equations (3.15), (3.16) and (3.19) with the defining equations (3.18) for f^{mn} :

$$G^{00} = K\frac{\frac{1}{\pi}\varphi_0\xi(\infty,1)KK_1(K) + KF^{00}(K)}{K + C(K)\cdot\cosh K}; \quad G^{10} = K\frac{F^{10}(K)}{K + C(K)\cosh K}$$

$$G^{01} = -\frac{F^{01}(K)}{K + S(K)\sinh K}; \quad G^{11} = K\frac{F^{11}(K)}{K + S(K)\sinh K} \qquad K \geq 0 \qquad (3.20)$$

It is easy to show that $G^{mn}(k)$ are continuous if $F^{mn}(k)$ are.

Now the corrections can be expressed in their final form

$$\Delta M_0 = M_0\frac{1 + \frac{\gamma-1}{2}M_0^2}{\sqrt{1-M_0^2}}\frac{1}{2}\varphi_0\xi(\infty,1) + \int_0^\infty F^{10}(K)\left(1 - \frac{\varepsilon_1\delta K}{1-M_0^2}\right)e^{-K}dK$$

$$\Delta\alpha_0 = -\frac{M_0^2}{M_\infty^2}\int_0^\infty F^{01}(K)\cdot\left(1 - \frac{\varepsilon_1\delta K}{1-M_0^2}\right)e^{-K}dK \qquad (3.21)$$

and so can the test quantities of equation (3.14) :

$$\frac{D}{D\xi}[\Delta M_0] = M_0\frac{1 + \frac{\gamma-1}{2}M_0^2}{\sqrt{1-M_0^2}}\int_0^\infty\left[\frac{1}{\pi}\varphi_0\xi(\infty,1)KK_1(K) + KF^{00}(K)\right]\left(1 - \frac{\varepsilon_1\delta K}{1-M_0^2}\right)e^{-K}dK$$

$$\frac{D}{D\xi}[\Delta\alpha_0] = \frac{M_0^2}{M_\infty^2}\int_0^\infty F^{11}(K)K\left(1 - \frac{\varepsilon_1\delta K}{1-M_0^2}\right)e^{-K}dK \qquad (3.22)$$

[+]The factor $\xi/\sqrt{\xi^2+1}$ in the expression for f^{00} has been introduced to avoid F^{00} becoming the Fourier transform of a discontinuous function.

3.4 Circular test section

To describe the flow in a circular test section we introduce polar coordinates x, r, Θ as defined in Figure 5. The plane $\Theta = 0$ and π coincides with the plane of symmetry of the flow ($z = 0$). The radius of the test section is the unit of length.

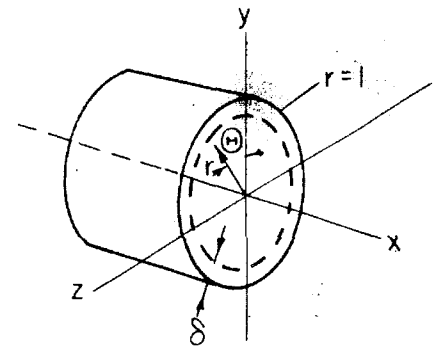

Fig. 5. Circular test section

The thickness δ of the boundary layer is taken to be constant. The model is situated at the x-axis, thus permitting the origin to be taken as characteristic point for zero perturbation.

For determining the wall interference potential $\varphi_w(x,r,\Theta)$ we have at our disposal the following equations:

$$
\left.
\begin{aligned}
&(1-M_0^2)\varphi_{wxx} + \varphi_{wrr} + \frac{1}{r}\varphi_{wr} + \frac{1}{r^2}\varphi_{w\Theta\Theta} = 0 \qquad \text{for } r<1 \\
&x \to -\infty: \quad \varphi_{wx} = -\frac{1}{1+\frac{\gamma-1}{2}M_0^2}\,\frac{\Delta M_0}{M_0}, \quad \varphi_{wr} = -\frac{M_\infty^2}{M_0^2}\Delta\alpha_0 \cos\Theta \\
&\qquad\qquad \frac{1}{r}\varphi_{w\Theta} = \frac{M_\infty^2}{M_0^2}\Delta\alpha_0 \sin\Theta \\
&x \to \infty: \quad \varphi_{wxx} = 0, \quad \varphi_{wxr} = 0, \quad \frac{1}{r}\varphi_{wx\Theta} = 0 \\
&r = 1: \quad \left[\frac{\partial}{\partial r} - \varepsilon_1\delta\left(\frac{\partial^2}{\partial x^2} + \frac{\partial^2}{\partial\Theta^2}\right) + \frac{1}{2}\varepsilon_2\delta^2\left(\frac{\partial^2}{\partial x^2} - \frac{\partial^2}{\partial\Theta^2}\right)\right](\varphi_w + \varphi_\infty) = 0 \\
&x = r = 0: \quad \varphi_w = 0, \quad \varphi_{wx} = 0, \quad \varphi_{wr} = 0, \quad \lim \frac{1}{r}\varphi_{w\Theta} = 0
\end{aligned}
\right\} \qquad (3.23)
$$

The potential $\varphi_\infty(x,r,\Theta)$ for the unbounded flow is assumed to be given at the walls as a Fourier series in Θ ($\xi = x/\sqrt{1-M_0^2}$):

$$
\varphi_\infty = \frac{\sqrt{1-M_0^2}}{1+\frac{\gamma-1}{2}M_0^2}\,\frac{\Delta M_0}{M_0}\,\xi + \frac{M_\infty^2}{M_0^2}\Delta\alpha_0\, r\cos\Theta + \sum_{n=0}^{\infty}\left[g^{0n}(\xi,r) + g^{1n}(\xi,r)\right]\cos n\Theta \qquad (3.24)
$$

The coefficients g^{mn} are even with respect ξ for $m = 0$ and odd for $m = 1$.

Similarly φ_w will be written in the form

$$\varphi_w = -\frac{\sqrt{1-M_0^2}}{1+\frac{\varkappa-1}{2}M_0^2}\,\frac{\Delta M_0^2}{M_0}\,\xi - \frac{M_\infty^2}{M_0^2}\,\Delta\alpha_0\, r\cos\theta +$$

$$+\sum_{n=0}^{\infty}\left[h^{0n}(\xi,r)+h^{1n}(\xi,r)\right]\cos n\theta,\quad 0\le r<1 \tag{3.25}$$

where the coefficients h^{mn} have the same symmetry as g^{mn}. The possibility of the developments (3.24) and (3.25) is evident from the assumptions initially made for φ_∞ and φ_w.

The functions $h^{mn}(\xi,r)$ are harmonic for $r<1$. In particular they can be developed in power series with respect to r, from which it is readily concluded that $h^{mn} = O(r^n)$ at the ξ-axis. Thus all functions h^{mn} for $n > 1$ are seen to disappear from the condition at $x = r = 0$ of equation (3.23). But the functions h^{mn} for $n \le 1$ should be independent of all functions g^{mn} for $n > 1$. Consequently it is sufficient in the correction problem to consider only the four unknown functions h^{mn} and h^{ml} as determined by g^{mo} and g^{ml}. The analogy with the plane case is evident, and we therefore can proceed rapidly towards the solution.

Corresponding to equations (3.11) and (3.12) in the plane case we obtain for h^{mn} ($m,n = 0$ and 1) the following boundary value problem within the half cylinder $r = 1$, $0 \le \xi < \infty$:

$$h^{mn}_{\xi\xi} + h^{mn}_{rr} + \frac{1}{r}h^{mn}_r - \frac{n^2}{r^2}h_{mn} = 0$$

$$\xi\to\infty:\quad h^{00}_\xi = h^{10}_\xi = \frac{2(1-M_0^2)}{1-M_0^2+2\varepsilon_1\delta-\varepsilon_2\delta^2}\int_0^\infty g_r^{00}(\xi,1)\,d\xi,\quad h^{01}=h^{11}$$

$$h^{01}_\xi = h^{11}_\xi = 0 \tag{3.26}$$

$$
\left.
\begin{aligned}
&\xi = 0 : \quad h^{0n}_{\xi} = 0, \quad h'^{n} = 0 \\
&r = 1 : \quad \left[\frac{\partial}{\partial r} - \varepsilon_1\delta\left(\frac{1}{1-M_0^2}\frac{\partial^2}{\partial\xi^2} - n^2\right) + \frac{1}{2}\varepsilon_2\delta^2\left(\frac{1}{1-M_0^2}\frac{\partial^2}{\partial\xi^2} + n^2\right)\right] \\
&\qquad\qquad (h^{mn} + g^{mn}) = 0 \\
&r = 0 : \quad h_r^{m0} = 0, \quad h^{m1} = 0
\end{aligned}
\right\} \qquad (3.26)\ \text{cont'd.}
$$

To estimate g^{mn} for large values of $R^2 = \xi^2 + r^2$ we note to begin with that $g^{01}(\infty,r) = g^{11}(\infty,r)$ since there is no upstream counterpart to the trailing vortices. For $r > 0$ the following estimates are available:

$$
\left.
\begin{aligned}
&g^{00} = O\left(\frac{1}{R}\right) \\
&g^{10} = O\left(\frac{\xi}{R^3}\right) \\
&g^{01}_{\xi} = O\left(\frac{\xi r}{R^5}\right) \\
&g^{11} = O\left(\frac{1}{r}\frac{\xi}{R}\right)
\end{aligned}
\right\} \qquad (3.27)
$$

They correspond to a source at the origin (g^{00}), a dublet at the origin with the axis in the ξ-direction (g^{10}), a uniform distribution along the ξ-axis of doublets in the y-direction plus a discrete one at the origin (g^{01}), and finally a distribution, uniform on each half of the ξ-axis, of doublets in the y-direction (g^{11}). It follows from the last of the estimates that

$$
g^{01}(\infty, r) = g^{11}(\infty, r) = g^{11}(\infty, 1)\frac{1}{r} \qquad (3.28)
$$

To arrive at a complete separation of the problems for h^{mn} we have to determine $h^{11}(\infty,r)$. Since $h^{11}_{\xi}(\infty,r) = 0$ and $g^{11}_{\xi}(\infty,r) = 0$ the problem (3.26) for h^{11} in the Trefftz plane reduces to

$$
\left.
\begin{aligned}
&h''_{rr} + \frac{1}{r}h''_r - \frac{1}{r^2}h'' = 0 \\
&r = 1 : \left(\frac{\partial}{\partial r} + \varepsilon_1\delta + \frac{1}{2}\varepsilon_2\delta^2\right)(h'' + g'') = 0 \\
&r = 0 : \quad h'' = 0
\end{aligned}
\right\}
$$

with the solution

$$h^{11}(\infty, r) = \frac{1 - \varepsilon_1\delta - \frac{1}{2}\varepsilon_2\delta^2}{1 + \varepsilon_1\delta + \frac{1}{2}\varepsilon_2\delta^2} g^{11}(\infty, 1)\, r \tag{3.29}$$

It is evidently possible to express the function g^{mn} in the neighborhood of $r = 1$ by means of continuous Fourier kernels as follows:

$$\left.\begin{aligned} g^{00}_{\xi\xi} &= \int_0^\infty G^{00}(K)\, \frac{K_0(rK)}{K_0(K)} \cos \xi K\, dK \\ g^{10}_{\xi} &= \int_0^\infty G^{10}(K)\, \frac{K_0(rK)}{K_0(K)} \cos \xi K\, dK \\ g^{01} &= \frac{g^{01}(\infty, 1)}{r} + \int_0^\infty G^{01}(K)\, \frac{K_1(rK)}{K_1(K)} \cos \xi K\, dK \\ g^{11}_{\xi} &= \int_0^\infty G^{11}(K)\, \frac{K_1(rK)}{K_1(K)} \cos \xi K\, dK \end{aligned}\right\} \tag{3.30}$$

The kernels are exponentially decreasing for $\xi \to \infty$, and in addition $G^{mo} = O(k^2)$ and $G^{m1} = O(|k|)$ for $k \to 0$. Hence the following solutions are easily verified:

$$\left.\begin{aligned} h^{00}_{\xi\xi} &= \int_0^\infty \frac{G^{00}(K)}{K^2} C(K) I_0(rK) \cos \xi K\, dK \\ h^{10}_{\xi} &= \frac{2(1 - M_0^2)}{1 - M_0^2 + 2\varepsilon_1\delta - \varepsilon_2\delta^2} \int_0^\infty g_r^{00}(\xi, 1)\, d\xi + \int_0^\infty \frac{G^{10}(K)}{K^2} C(K) I_0(rK) \cos \xi K\, dK \\ h^{01} &= \frac{1 - \varepsilon_1\delta - \frac{1}{2}\varepsilon_2\delta^2}{1 + \varepsilon_1\delta + \frac{1}{2}\varepsilon_2\delta^2} g^{01}(\infty, 1) \cdot r + \int_0^\infty \frac{G^{01}(K)}{K} S(K) \frac{I_1(rK)}{K} \cos \xi K\, dK \\ h^{11} &= \int_0^\infty \frac{G^{11}(K)}{K} S(K)\, \frac{I_1(rK)}{K} \cos \xi K\, dK \end{aligned}\right\} \tag{3.31}$$

where

$$C(K) \equiv -\frac{K^2}{K_0(K)} \cdot \frac{(1-M_0^2)K_0'(K) + (\varepsilon_1\delta - \frac{1}{2}\varepsilon_2\delta^2)K K_0(K)}{(1-M_0^2)I_0'(K) + (\varepsilon_1\delta - \frac{1}{2}\varepsilon_2\delta^2)K I_0(K)}$$

$$S(K) \equiv -\frac{K^2}{K_1(K)} \cdot \frac{(1-M_0^2)\left[K_1'(K) + (\varepsilon_1\delta + \frac{1}{2}\varepsilon_2\delta^2)K_1(K)\right] + (\varepsilon_1\delta - \frac{1}{2}\varepsilon_2\delta^2)K^2K_1(K)}{(1-M_0^2)\left[I_1'(K) + (\varepsilon_1\delta + \frac{1}{2}\varepsilon_2\delta^2)I_1(K)\right] + (\varepsilon_1\delta - \frac{1}{2}\varepsilon_2\delta^2)K^2 I_1(K)} \qquad (3.32)$$

The functions C(k) and S(k) are everywhere continuous since $\varepsilon_1\delta > \varepsilon_2\delta^2 > 0$, and for k large they decrease like $k^{3/2}e^{-k}$.

We now introduce the pressure distribution at the wall by writing

$$\varphi_{0\xi}(\xi, 1, \theta) = \sum_{m,n} f^{mn}(\xi)\cos n\theta, \quad f^{mn}(\xi) \equiv g_\xi^{mn}(\xi, 1) + h_\xi^{mn}(\xi, 1) \qquad (3.33)$$

where the coefficients f^{mn} are taken to be given in the form

$$\begin{aligned}
f^{00}(\xi) &= \tfrac{1}{2}\varphi_{0\xi}(\infty, 1, \tfrac{\pi}{2})\frac{\xi}{\sqrt{\xi^2+1}} + \int_0^\infty F^{00}(K)\sin\xi K\, dK \\
f^{10}(\xi) &= \tfrac{1}{2}\varphi_{0\xi}(\infty, 1, \tfrac{\pi}{2}) + \int_0^\infty F^{10}(K)\cos\xi K\, dK \\
f^{01}(\xi) &= \int_0^\infty F^{01}(K)\sin\xi K\, dK \\
f^{11}(\xi) &= \int_0^\infty F^{11}(K)\cos\xi K\, dK
\end{aligned} \qquad (3.34)$$

The functions $G^{mn}(k)$ then can be expressed by the Fourier transforms F^{mn} as follows:

$$G^{00} = K^2\frac{\frac{1}{\pi}\varphi_{0\xi}(\infty, 1, \frac{\pi}{2})K K_1(K) + K F^{00}(K)}{K^2 + C(K)I_0(K)}; \quad G^{10} = K^2\frac{F^{10}(K)}{K^2 + C(K)I_0(K)}$$

$$G^{01} = -K\frac{F^{01}(K)}{K^2 + S(K)I_1(K)}; \qquad G^{11} = K^2\frac{F^{11}(K)}{K^2 + S(K)I_1(K)} \qquad K\geq 0 \qquad (3.35)$$

and the corrections are obtained in their final form:

$$
\left.
\begin{aligned}
\Delta M_o &= M_o \frac{1+\frac{\gamma-1}{2}M_o^2}{\sqrt{1-M_o^2}} \left\{ \frac{1}{2}\bar{\varphi}_{o\xi}(\infty,1,\tfrac{\pi}{2}) + \int_o^\infty F^{10}(K)\left[KK_1(K) - \frac{\varepsilon_1\delta - \frac{1}{2}\varepsilon_2\delta^2}{1-M_o^2} K^2 K_o(K)\right] dK \right\} \\
\frac{D}{D(\xi)}\left[\Delta M_o\right] &= M_o \frac{1+\frac{\gamma-1}{2}M_o^2}{\sqrt{1-M_o^2}} \int_o^\infty \left[\frac{1}{\pi}\bar{\varphi}_{o\xi}(\infty,1,\tfrac{\pi}{2}) KK_1(K) + KF^{00}(K)\right]\left[KK_1(K) - \right. \\
&\qquad \left. - \frac{\varepsilon_1\delta - \frac{1}{2}\varepsilon_2\delta^2}{1-M_o^2} K^2 K_o(K)\right] dK \\
\Delta\alpha_o &= \frac{M_o^2}{M_\infty^2}\left\{ (1-\varepsilon_1\delta - \tfrac{1}{2}\varepsilon_2\delta^2)\int_o^\infty f''(\xi)\,d\xi - \frac{1}{2}\int_o^\infty \frac{F^{01}(K)}{K}\left[K^2K_o(K) + (1-\varepsilon_1\delta - \tfrac{1}{2}\varepsilon_2\delta^2 - \right. \right. \\
&\qquad \left. \left. - \frac{\varepsilon_1\delta - \frac{1}{2}\varepsilon_2\delta^2}{1-M_o^2}) KK_1(K)\right] dK \right\} \\
\frac{D}{D\xi}(\Delta\alpha_o) &= \frac{1}{2}\frac{M_o^2}{M_\infty^2}\int_o^\infty F''(K)\left[K^2K_o(K) + (1-\varepsilon_1\delta - \tfrac{1}{2}\varepsilon_2\delta^2 - \frac{\varepsilon_1\delta - \frac{1}{2}\varepsilon_2\delta^2}{1-M_o^2}) KK_1(K)\right] dK
\end{aligned}
\right\} \quad (3.36)
$$

3.5 Numerical examples

To get an idea of the boundary layer influence on the corrections a few typical examples have been investigated. For simplicity the perturbation potentials g^{mn} for unbounded flow are assumed to be know rather than the pressure distributions f^{mn}, which should be used in practice.

The theory developed offers approximate solutions when the wall boundary layers are thin. The first example of plane flow serves to indicate the maximum thickness for which the approximation is good. This is achieved by comparison with a case for which accurate solutions are available, to be specific the case of constant undisturbed Mach number $M(< M_o)$ in the boundary layer. In Reference 9 such solutions have been obtained for the subsonic flow around symmetrical parabolic arc profiles when the boundary layer profile

is the following:

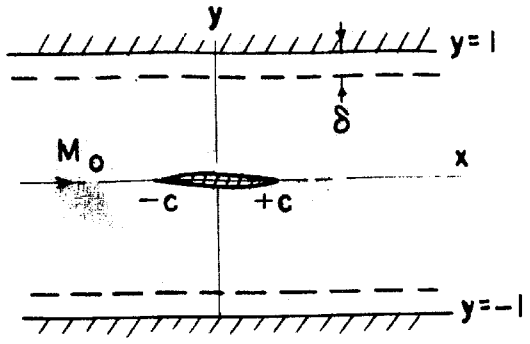

Fig. 6. Symmetric parabolic arc profile.

$$M = \begin{cases} \frac{M_o}{2}\sqrt{2} & \text{for } 1-\delta \le |Y| < 1 \\ M_o & \text{for } |Y| < 1-\delta \end{cases} \qquad (3.37)$$

For this profile one has $\mathcal{E}_1 = 1$, which value is to be used in comparing accurate and approximate solutions.

The functions g^{mn} of the first plane example accordingly corresponds to the subsonic flow[+] around a symmetric parabolic arc profile at zero angle of attack (see Figure 6). Only g^{10} is different from zero; the associated Fourier transform as defined by equation (3.15) is

$$G^{10}(K) = |K|\, G\left(\frac{cK}{\sqrt{1-M_o^2}}\right) e^{-|K|}; \qquad G(q) \equiv \frac{\sin q - q\cos q}{q^3} \qquad (3.38)$$

where $2c$ is the length of the chord[++].

As a typical value is taken $c = 1/4$ with half of the tunnel height as unit of length. Figure 15 shows how the computed values of the correction ΔM_o depend upon the boundary layer thickness for some values of M_o. The full curves were obtained by the approximate theory while the broken curves - taken from Reference 9 - give the accurate result for the specific boundary layer profile of equation (3.37). One concludes that in the present case the approximation for thin boundary layers is good for $\delta < 0.1$ and reasonable for $0.1 < \delta < 0.2$ Thicker boundary layers are not likely to occur in practice.

[+] A given set of functions g^{mn} can be made to produce a subsonic field by taking the relative thickness τ of the model sufficiently small. Since the theory is linear g^{mn} and τ will decrease in the same proportion. Equation (3.38) corresponds to $\tau = \frac{\pi}{4}(1-M_o^2)/c^2$.

[++] Note that $G(q)$ is continuous at $q = 0$.

The influence of the wall boundary layers as shown by Figure 15 for the specific case under consideration will be seen to have as essentially universal character+. From the value at $\delta = 0$ ΔM_o decreases with increasing δ. For $M_\infty = 0.85$ the boundary layer thickness $\delta = 0.2$ (for $\varepsilon_1 = 1/2$) brings ΔM_o down to half the initial value, and for higher Mach numbers still thinner boundary layers are sufficient to produce this effect. For $M_o = 0.95$ the thickness $\delta = 0.3$ gives $\Delta M_o = 0$. Roughly speaking the thickness required for reduction by half is of the order $\delta = 0.8\,(1-M_o^2)$ and for complete reduction $\delta = 2.5(1-M_o^2)$. Altogether there is a considerable influence of the boundary layers in the range of practically attainable values of δ.

From Reference 9 it can be concluded that the influence just discribed does not change appreciably with the length of the chord. However, for long models ΔM_o is not independent of the choice of representative point. This is evident from Figure 16, where ΔM_o at $M_o = 0.90$ as a function of $\varepsilon_1\delta$ has been plotted for two different chord lengths (c=0.25 and 0.375) and two different representative points (leading edge and mid-chord). The important conclusion to be drawn from Figure 16 (and from other results of Reference 9) is that the variation of ΔM_o with the position of the representative point is almost cancelled for a certain boundary-layer thickness, which is of the same order of magnitude as that required for reducing ΔM_o to half its value for $\delta = 0$.

To be able to discuss in simple terms more general types of plane models, we note that if the estimates (3.9) for g^{mn} are taken to be valid everywhere at the wall then there is a very simple relationship

---

+The correction ΔM_o has been divided by its value for $\delta = 0$. This normalization is thought to bring out the essential features of the boundary layer influence even when linear theory cannot be used to determine ΔM_o from the form and size of the model.

between the transforms $G^{mn}(k)$:

$$G^{00} \propto G^{10} \propto |K| G^{01} \propto |K| G^{11} (\propto |K| e^{-|K|}) \tag{3.39}$$

When in practice the chord and the transonic region are not small enough to make the estimates good, the difference involved may roughly be thought of as a common change of length scale for the functions g^{mn} at the central part of the wall. The relations (3.39) then remain approximately valid.

Thus taking $G^{00} \propto G^{10}$ the results for our specific choice (3.38) of G^{10} may be reinterpreted. From comparing equations (3.13), (3.14) and (3.16) it becomes evident that the curves of Figures 15 and 16 might as well be taken to represent the boundary layer influence on the correction gradient $\frac{D}{D\xi}[M_o]$. In this connection one should remember that $\frac{D}{D\xi}[M_o]$ is large for halfbodies[+] while for finite bodies it is essentially due to the wake and consequently is small[++]. The same is of course true for the g^{00} contribution to ΔM_o (see equation (3.16)). For a plane halfbody with negligible g^{10} one simply has

$$\frac{\Delta M_o}{[\Delta M_o]_{\delta=0}} = \frac{1}{1+\frac{\varepsilon_1 \delta}{1-M_o}} \tag{3.40}$$

This relationship has been plotted in Figure 17, from which it is seen that the boundary layer influence on the Mach number correction is not quite as strong for a halfbody as for a finite body, although it has the same general character.

Finally in the case of a lifting profile we choose as a typical example

$$G^{01} = G^{11} = G\left(\frac{cK}{\sqrt{1-M_o^2}}\right) e^{-|K|}; \qquad c = 1/4 \tag{3.41}$$

following equations (3.38) and (3.39). The resulting corrections are plotted

---

[+] A halfbody is understood to extend to downstream infinity as a cylinder parallel to undisturbed flow.

[++] Except when the flow is highly separated.

in Figure 18 - the boundary layer influence being identically the same for $\Delta\alpha_o$ and $\frac{D}{D\xi}[\Delta\alpha_o]$. The difference between corresponding curves of Figures 15 and 18 is remarkably small. Thus the boundary layer influence in plane flow follows a universal pattern independent of thickness distribution, angle of attack, or camber.

Turning now to the three-dimensional case we choose $G^{oo} = 0$ and

$$G^{10}(K) = K^2 H\left(\frac{cK}{\sqrt{1-M_o^2}}\right) K_o(K) \quad , \qquad H(q) \equiv \frac{(3-q^2)\sin q - 3q\cos q}{q^5} \tag{3.42}$$

(where H (q) is continuous at q = 0). In subsonic flow having rotational symmetry this choice corresponds to a symmetrical body of revolution with a parabolic contour (as in Figure 6). For $c = 0.4$ the Mach number correction ΔM_o is found to depend upon the boundary layer thickness[+] as shown by Figure 19. There is no essential difference from the corresponding plane case, only the boundary layer influence is slightly smaller for large values of δ. The thickness required for reduction by half is $\delta \simeq 0.7\ (1-M_o^2)$ and for complete reduction $\delta \simeq 4.4\ (1-M_o^2)$.

Even in three dimensions it makes sense to interchange the assumed forms for G^{oo} and G^{10} when considering a halfbody instead of a finite body. Thus Figure 19 can be interpreted as showing the boundary layer influence on $\frac{D}{D\xi}(\Delta M_o)$. For the Mach number correction one obtains the simple result

$$\frac{\Delta M_o}{[\Delta M_o]_{\delta=0}} = \frac{1-M_o^2}{1-M_o^2+2\varepsilon_1\delta-\varepsilon_2\delta^2} \tag{3.43}$$

which has been plotted in Figure 20. The influence is twice as large as in the plane case.

When a three-dimensional model carries lift the interference picture is somewhat complicated by the presence of trailing vortices. However, the

---

[+]Note that the δ^2-term, arising from the wall curvature, is negligible in Figures 19 to 21.

interference due to lift as calculated by linear theory remains small even for $M_o \to 1$ in contrast to the blockage interference. Furthermore the contributions of G^{01} and G^{11} to $h^{01}(0,0)$ and $h^{11}(0,0)$ in equation (3.31) are negligible except for exceptionally long models (see Reference 27) and in addition they are expected to decrease with increasing δ in much the same way as in the plane case. All in all it seems sufficient to consider only the "lifting-line correction" $\Delta\alpha_o$ obtained from the $g^{01}(\infty,1)$-term of equation (3.31). The simple result is

$$\frac{\Delta\alpha_o}{[\Delta\alpha_o]_{\delta=0}} = \frac{1-\varepsilon_1\delta-\frac{1}{2}\varepsilon_2\delta^2}{1+\varepsilon_2\delta+\frac{1}{2}\varepsilon_2\delta^2} \tag{3.44}$$

which has been plotted in Figure 21. Thus the boundary layer influence on $\Delta\alpha_o$ is small and independent of M_o. Surprising as this result might be, it could have been anticipated from the fact that the pressure perturbation due to a lifting line has fore-and-aft symmetry (in linear approximation), permitting only crossflow but not streamwise changes in mass flow density to contribute to $\Delta\alpha_o$ (compare footnote to section 2.6).

IV. WALL INTERFERENCE AT CHOKING

4.1 Introduction

When the Mach number M_o in front of the model in a closed test section increases, the transonic region at the model readily comes so close to the walls that the linear correction theory is no longer applicable. If corrections exist at all at higher Mach numbers (compare paragraph 3.2) they seem to increase steadily until choking occurs.

Choking constitutes an upper limit M_{ch} to M_o :

$$M_o \leq M_{ch} < 1 \tag{4.1}$$

corresponding to the greatest possible mass flow through the test section. The flow field established has a section of sonic speed between the model and the wall. For a very small model compared to the test section, it seems reasonable to expect this flow field to approach, in the neighborhood of the model, the unbounded field for $M_\infty \longrightarrow 1^+$. Furthermore, there is some theoretical and experimental evidence to the effect that the choked flow field at the model may be interpreted as belonging to some unbounded field of Mach number M_∞ with

$$M_{ch} < M_\infty < 1 \tag{4.2}$$

even for reasonably large models (see for example References 21 and 22). If this is the case one might try to determine the correction $\Delta M_o = M_\infty - M_{ch}$. However, this would require comprehensive experiments or calculations, and therefore it might in practice be possible to consider only cases where $M_\infty \simeq 1$.

In the present chapter the correction problem for choked flow will be studied with special attention to the boundary layer influence. As a

---

+In fact, this hypothesis can be taken as a definition of sonic flow (see Reference 20).

basis will serve to a large extent theoretical results for sonic flow obtained by Guderley and his collaborators (References 20-26).

4.2 Unbounded sonic flow.

An essential feature of the flow about a simple body in an unbounded stream of sonic velocity is the existence of a surface with sonic velocity (the "sonic line") extending laterally from the model to infinity. The flow in the upstream region of this surface is subsonic, while it is supersonic in a downstream region bounded by one or more shocks (see Figure 7). The outgoing characteristic surfaces reach the sonic surface if they are far enough forward, otherwise they extend to infinity or reach the trailing shock system. The boundary between the two families of characteristic surfaces is called the limiting Mach wave. The flow in front of the limiting Mach wave is in principle independent of the form of the body behind it. For a simple body as shown by Figure 7 the limiting Mach wave seems to start at the body in front of the position of the maximum thickness.

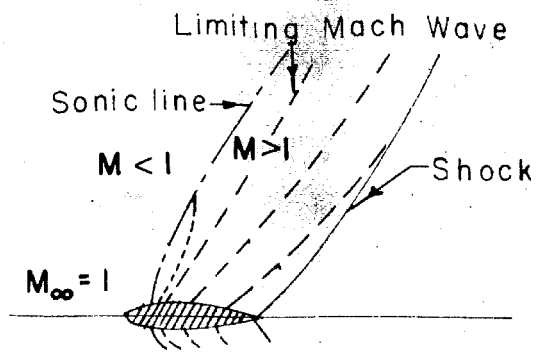

Fig. 7. Sonic flow

In subsonic flow the asymptotic field far from the body is easily obtained: corresponding to a halfbody one takes a source, and to a finite body a doublet, to be situated within the body, the strength being proportional to the cross sectional area or the volume of the body respectively. If the flow field at sonic velocity similarly can be approximated in a universal form there should, in a large part of the field, be no difference for the two body types, since those are different only behind the limiting

Mach wave. Now Guderley and his coworkers have found such a basic solution (or rather two solutions: one for plane flow and another for three-dimensional flow) using the classical transonic approximation[+]. A presentation follows next.

In the plane case let the basic perturbation potential be $\varphi_p(x,y)$, satisfying the differential equation

$$\frac{\partial^2\varphi}{\partial Y^2} = (\gamma+1)\frac{\partial\varphi}{\partial X}\frac{\partial^2\varphi}{\partial X^2} \tag{4.3}$$

The condition for universality is expressed by requiring φ_p to be similar to itself in the following sense. For all positive values of the parameter c it should be true that

$$\varphi_p[b(c)x, cy] = a(c)\varphi_p(x,y)$$

where a and b are continuous functions of c satisfying the transitivity conditions

$$\left.\begin{aligned} a(c_1)\,a(c_2) &= a(c_1 c_2) \\ b(c_1)\,b(c_2) &= b(c_1 c_2) \end{aligned}\right\}$$

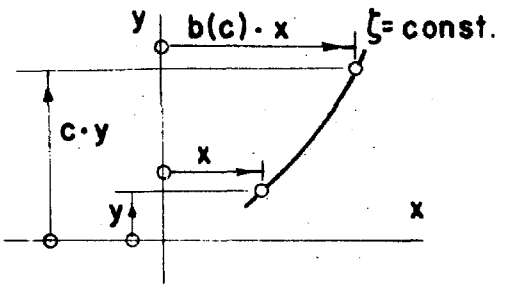

Fig. 8. Similarity pattern of basic solution

It follows that a and b have to be powers of c, and hence that the loci of similarly situated points, in the sense of the similarity introduced, have to satisfy equations of the form xy^{-n} = constant. One therefore introduces

$$\zeta \equiv (\gamma+1)^{-\frac{1}{3}} X Y^{-n} \tag{4.4}$$

as a new coordinate in order to determine φ_p in the form

$$\varphi_p(X,Y) = Y^m f_p(\zeta) \tag{4.5}$$

[+]It is, however, easy to show that the basic solutions are asymptotic solutions of the exact potential equation, thus providing a valuable verification of the transonic approximation.

Introduction of this expression into the differential equation (4.3) shows m to be $m = 3n - 2$, and $f_p(\zeta)$ to fulfill the following ordinary differential equation

$$(n^2\zeta^2 - f_p')f_p'' + 5n(1-n)\zeta f_p' - 3(1-n)(3n-2)f_p = 0 \qquad (4.6)$$

For the perturbation velocity to vanish at infinity n has to be smaller than unity.

The resulting problem then is to find such a solution of equation (4.6) that the corresponding flow field has the structure initially described. To begin with there should be a sonic line. Since the condition for sonic velocity is $f' = 0$, the sonic line has to be a curve ζ = constant, say $\zeta = \zeta_0$. For the sonic line to have the form required one must have $n > 0$, $\zeta_0 > 0$. For $\zeta < \zeta_0$ f_p' ought to be negative (i.e. subsonic upstream flow), while for $\zeta > \zeta_0$ positive values are expected (giving supersonic flow at least up to a limiting Mach wave).

In the supersonic region let an outgoing characteristic curve have the equation $y = Y(x)$. Its slope then is determined by

$$\frac{dY}{dx} = (\gamma+1)^{-1/3} Y^{1-n} \frac{1}{\sqrt{f_p'(\zeta)}}$$

For a curve ζ = constant the corresponding expression is

$$\frac{dY}{dx} = (\gamma+1)^{-1/3} Y^{1-n} \frac{1}{n\zeta}$$

Hence immediately behind the sonic line the outgoing characteristics cut across the curves ζ = constant in direction towards the sonic line and this remains true as long as $f_p' < n^2\zeta^2$. It might then be concluded that a limiting Mach wave ζ = constant is reached if $f_p = n^2\zeta^2$ for some value of ζ. Without loss of generality $\zeta = 1$ is chosen to be the limiting Mach wave, corresponding to selection of one specific solution out of the group generated according to the transonic similarity rule.

For the limiting Mach wave the differential equation (4.6) has a singular point. The solution must however be regular there, and it is seen that this condition determines a unique solution in a neighborhood of $\zeta = 1$ (for n given: $0 < n < 1$). Similarly for $\zeta \longrightarrow -\infty$ the condition $f_P' \rightarrow 0$ (zero perturbation velocity at infinity) determines a solution which is unique except for an arbitrary factor. By choosing the proper values for this factor and for the parameter n one finally is able to make the two solutions coincide and form, in the interval $-\infty < \zeta \leq 1$, the solution f_P required. The value $n = 4/5$ has been found to do the trick (References 23 and 24). The result for $f_P'(\zeta)$ ($\propto \varphi_{Px}$) is plotted in Figure 9. In Figure 10 is shown the deformation ΔY of the undisturbed streamline $y = Y$.

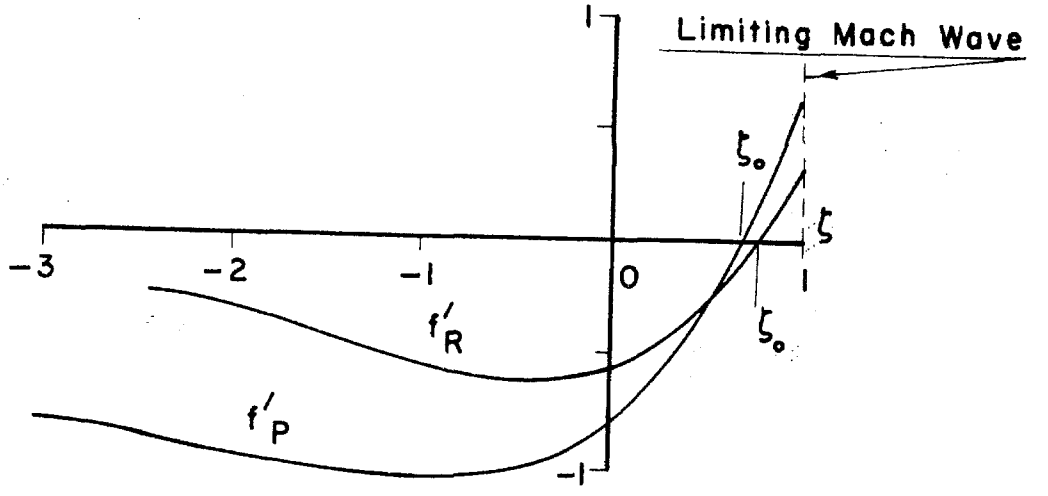

Fig. 9. Longitudinal perturbation velocity of basic solutions (C=1).

The same analysis can be performed in the case of rotational symmetry. One assumes the basic potential $\varphi_R(x,r)$, satisfying the equation

$$\frac{\partial^2 \varphi}{\partial r^2} + \frac{1}{r}\frac{\partial \varphi}{\partial r} = (\gamma+1)\frac{\partial \varphi}{\partial x}\frac{\partial^2 \varphi}{\partial x^2} \qquad (4.7)$$

to have the form

$$\varphi_R = r^{3n-2} f_R(\zeta); \qquad \zeta \equiv (\gamma+1)^{-1/3} x r^{-n} \tag{4.8}$$

A solution of the required type is obtained for $n = 4/7$[+] (Reference 25). The longitudinal velocity perturbation f_R and the streamline deformation ΔR for the undisturbed streamline $r = R$ are given in Figures 9 and 10.

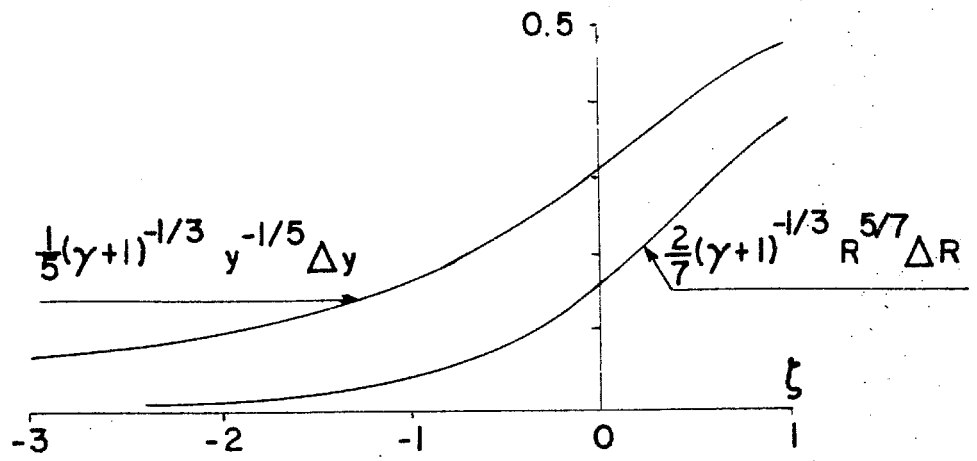

Fig. 10. Streamline shapes of basic solutions (C=1).

It is possible to continue f_P and f_R across $\zeta = 1$, but the result does not give undisturbed flow for $\zeta \to \infty$. This is of course related to the fact that one or more shocks are needed for the transition. It was shown in Reference 24 that it is possible to fit uniquely a shock along a surface ζ = constant in such a way that the perturbation velocity behind it continously approaches zero for $\zeta \to \infty$. It also seems possible to fit several shocks in the same way, although uniqueness then is lost. However, for the present problem the shock wave pattern will be seen to be unimportant.

The functions $f_p(\zeta)$ and $f_R(\zeta)$ combined with the transonic similarity rule give two groups of basic solutions depending upon a positive

---

[+]This value has been obtained by numerical integration of the differential equation for f_R, and it is therefore not necessarily exact (see Reference 24).

Parameter C in the following way:

$$\varphi_P(X,Y;C,\gamma) \equiv C^{-3} Y^{2/5} f_P\left[C(\gamma+1)^{-1/3} X Y^{-4/5}\right]$$
$$\varphi_R(X,r;C,\gamma) \equiv C^{-3} r^{-2/7} f_R\left[C(\gamma+1)^{-1/3} X r^{-4/7}\right] \qquad (4.9)$$

A fundamental hypothesis of Guderley's, and one to be extensively used here, assumes that the perturbation potential due to an arbitrary body at sonic speed is asymptotically given by the expressions (4.9) at a large distance from the body in front of the shock system. In the plane case φ_P and in the three-dimensional case (also without rotational symmetry) φ_R should be used, in any case with a suitably chosen value for C. Those sonic perturbation fields which are known - from computations or experiments - verify the hypothesis, and indicate the approximation to be good also so close to the body as wind tunnel walls may be situated at transonic tests (see Reference 22)+.

To arrive at a complete picture of the flow field far from the body - the asymptotic field - we must know how to determine the parameter C from the size and form of the body. Let us consider, to begin with, only families of affine symmetric bodies, the members of which are defined by a length c in the streamwise direction and a slenderness ratio τ, for example as indicated in Figure 11. If, in the plane case, the perturbation potential for $c = \tau = 1$, $\gamma = 0$ is $\bar{\varphi}(x,y)$, then the potential for

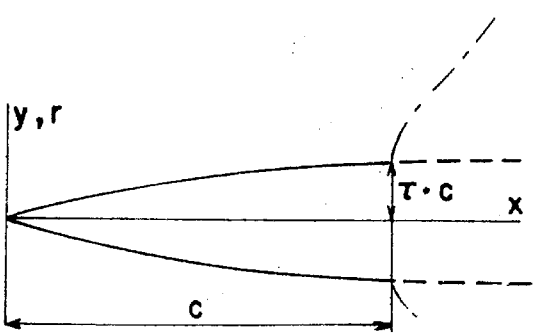

Fig. 11. Body parameters

+The approximation is of course not good when the walls really are situated there.

arbitrary values of c, τ and γ is[+]

$$\varphi(x,y) = c\tau^{2/3(\gamma+1)^{-1/3}}\bar{\varphi}\left[\frac{x}{c}, \tau^{1/3(\gamma+1)^{1/3}}\frac{y}{c}\right] \tag{4.10}$$

Let us furthermore assume that for $c = \tau = 1, \gamma = 0$ one has to choose $C = C_p$ inequation (4.9) to describe correctly the asymptotic field. We then have

$$\bar{\varphi}(x,y) \approx \varphi_p(x, y; C_p, 0)$$

and consequently

$$\varphi(x,y) \approx c\tau^{2/3(\gamma+1)^{-1/3}}\bar{\varphi}_p\left[\frac{x}{c}, \tau^{1/3(\gamma+1)^{1/3}}\frac{y}{c}; C_p, 0\right]$$

Hence one concludes that

$$\varphi(x,y) \approx \varphi_p(x,y; C, \gamma); \quad C = c^{-1/5}\tau^{-4/15(\gamma+1)^{1/15}}C_p \tag{4.11}$$

Similarly one obtains in the case of rotational symmetry (see Reference 28)

$$\varphi(x,r) = c\tau^2\bar{\varphi}\left[\frac{x}{c}, \tau(\gamma+1)^{1/2}\frac{r}{c}\right] \tag{4.12}$$

and

$$\varphi(x,r) \approx \varphi_R(x,r; C, \gamma); \quad C = c^{-3/7}\tau^{-4/7(\gamma+1)^{1/21}}C_R \tag{4.13}$$

where $\bar{\varphi}$ and C_R correspond to $c = \tau = 1, \gamma = 0$ (see Figure 11).

From equations (4.11) and (4.13) it is seen that affine bodies have the same asymptotic fields if they have equal values for $c\tau^{4/3}$[++]. Now Barish (Reference 22) has made it likely that in the plane case this conclusion is valid also for arbitrary symmetrical bodies (i.e. not necessarily affine) if c and τ refer to that part of the body which is in front of the point of sonic velocity as shown in Figure 11. Hence there seems to be a more or less universal value of C_p for symmetrical bodies[+++]; data in Reference 22 give $C_p = 1.15$. However, the difficult problem of

---

[+] Here the boundary condition for the body is assumed to be specified on both sides of the x-axis, not at the contour.

[++] For halfbodies at subsonic speed the corresponding condition is $c\tau$ = constant.

[+++] Restricted of course to bodies which are thin enough for the transonic approximation and the simplified boundary condition at the model to be valid.

finding the point of sonic velocity remains.

In the axisymmetric case the information available is not sufficient to decide whether or not C_R is independent of the form of the body for the special choice of c and τ. One specific body investigated in Reference 25 has $C_R \simeq 0.9$.

Using these values of C_P and C_R one should be able to estimate the asymptotic fields of profiles and three-dimensional bodies when they are symmetrical with respect to the x-axis. The restriction to symmetrical flow may not be too important however. In Reference 26 the influence of asymmetry on the asymptotic field was investigated in the plane case, and it was found to be negligible as long as the angle of attack and camber are much smaller than the slenderness ratio τ. In the three-dimensional case the restriction is still smaller. It was stressed by Oswatitsch in Reference 29 that three-dimensional transonic fields show a very strong trend towards rotational symmetry once one is outside the immediate neighborhood of the body[+]. He therefore proposed to consider the outer field as generated by a fictitious body of revolution along the x-axis - the "equivalent body of revolution". The problem of determining the asymptotic field of an arbitrary body thus is the same as that of finding its equivalent body of revolution. For slender bodies, like delta wings of small aspect ratio, the equivalent body of revolution is obtained by changing each cross section x = constant into a circle of unchanged area[++].

4.3 Asymptotic fields at choking

Turning now to the case of choking, we consider the plane flow about a

---

[+] The same trend also appears at high subsonic speeds as shown in Reference 30.

[++] This should be viewed against the fact that linear theory gives finite values at $M_\infty = 1$ for the influence of such changes of the body form which leave invariant the distribution of cross-sectional area.

model which is symmetrically situated in a wind tunnel with the walls at $y = \pm 1$. At blockage there is a sonic line and a limiting Mach wave between the model and a common point at the wall (see Figure 12). As long as the model is sufficiently small it is to be expected that the flow field in a neighborhood of the model nearly coincides with the unbounded field for $M_\infty = 1$. At the outer boundary of this neighborhood it should be possible to approximate the perturbation potential by $\varphi_p(x,y;C,\gamma)$ according to equation (4.9) with a suitable value for C. The problem of finding an asymptotic approximation for the choked flow around a small model then reduces to the problem of finding a basic solution $\Phi_p(x,y;C,\gamma)$ of equation (4.3) (regular from upstream infinity to the limiting Mach wave), which for $x,y \to 0$ in some sense approaches $\varphi_p(x,y;C,\gamma)$, and at the wall ($y = \pm 1$) satisfies the condition $\frac{\partial}{\partial Y}\Phi_P = 0$.

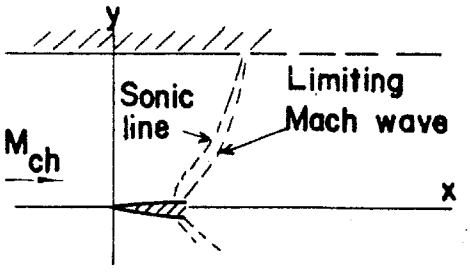

Fig. 12. Flow at choking

Assuming that such a solution exists we write it for $C = 1$ in the form

$$\Phi_p(X,Y;1,\gamma) = F_p(Y,\xi) \tag{4.14}$$

where ξ is defined by equation (4.9). For arbitrary values of C the solution then is

$$\Phi_p(X,Y;C,\gamma) = C^{-3} F_p\left[Y,\ C(\gamma+1)^{-1/3} \times Y^{-4/5}\right] \tag{4.15}$$

as is evident from a comparison with equation (4.4).

The same approach in the axisymmetric case leads to the following form for a basic perturbation potential Φ_R which (with the wall at $r = 1$) equals φ_R at the origin:

$$\Phi_R(X,r;C,\gamma) = C^{-3} F_R\left[r,\ C(\gamma+1)^{-1/3} \times r^{-4/7}\right] \tag{4.16}$$

Far upstream the potentials ϕ_P and ϕ_R ought to give uniform subsonic flow of Mach number M_{ch}, the condition for this being that the ξ - derivatives of F_P and F_R be finite and proportional to $y^{4}/5$ and $r^{4}/7$ respectively for $\xi \to -\infty$. We therefore assume the existence of the following limits for $\xi \to -\infty$:

$$\left.\begin{aligned} &\lim\, y^{-4/5}\, \frac{\partial}{\partial \xi} F_P(Y,\xi) = F_P^{\infty} \\ &\lim\, r^{-4/7}\, \frac{\partial}{\partial \xi} F_R(r,\xi) = F_R^{\infty} \end{aligned}\right\} \qquad (4.17)$$

The constants F_P^{∞} and F_R^{∞} thus defined are negative since they give M_{ch} - which is smaller than one - by the following expressions:

$$M_{ch} = \begin{cases} 1 + \frac{1}{2}(\gamma+1)^{2/3}\, C^{-2} F_P^{\infty} \\ 1 + \frac{1}{2}(\gamma+1)^{2/3}\, C^{-2} F_R^{\infty} \end{cases} \qquad (4.18)$$

Using equations (4.11) and (4.13) to express C in terms of the model parameters, one obtains for the choking Mach number in the plane case

$$M_{ch} = 1 + \frac{1}{2} c_P^{-2} F_P^{\infty} (\gamma+1)^{\frac{1}{2}} (\tau c)^{\frac{1}{2}} \left[c\, \tau^{-1/3} (\gamma+1)^{-1/3} \right]^{-1/10} \qquad (4.19)$$

and in the three-dimensional case

$$M_{ch} = 1 + \frac{1}{2} c_R^{-2} F_R^{\infty} (\gamma+1)^{1/2} \tau c \left[c\, \tau^{-1} (\gamma+1)^{-1/2} \right]^{-1/7} \qquad (4.20)$$

The result, which essentially is due to Guderley (Reference 21) shows how the choking Mach number depends upon the size and form of the model when this is small. The corresponding result for a large model, obtained by one-dimensional theory (see Reference 5), is

$$M_{ch} = 1 - \left(\frac{\gamma+1}{2}\right)^{\frac{1}{2}} (\tau c)^{\frac{1}{2}}$$

in plane flow, and

$$M_{ch} = 1 - \left(\frac{\gamma+1}{2}\right)^{\frac{1}{2}} \tau c$$

in three-dimensional flow. Here c and τ still are defined with respect to the sonic point (see Figure 11), which however has moved downstream to the position of the maximum thickness. It follows from the transonic similarity rules (see equations 4.10 and 4.12) that $c\tau^{-1/3}(\gamma+1)^{-1/3}$ and $c\tau^{-1}(\gamma+1)^{1/2}$ are the characteristic lengths for deciding, in the plane and three-dimensional cases respectively, whether a given model is small or large enough for the approximate expressions for M_{ch} to be valid. Only small powers of the characteristic lengths are seen to contribute to the difference in form between the expressions, so the influence of chord length on M_{ch} may still be small (for τ c fixed).

The discussion of asymptotic fields at choking is readily extended to include the influence of thin wall boundary layers. Let us for a change begin with the three-dimensional case. As boundary condition for the perturbation potential at the wall (r = 1) we have from equation (2.23)

$$\frac{\partial \varphi}{\partial r} = \vartheta \frac{\partial^2 \varphi}{\partial x^2}, \qquad \vartheta = \varepsilon_1 \delta - \tfrac{1}{2}\varepsilon_2 \delta^2 \tag{4.21}$$

It is important that this boundary condition - as well as the corresponding one for plane flow - permits transonic similarity (as was shown in Section 2.6), since we are using similarity arguments extensively.

We are led to ask for a basic solution $\Phi_R(x,r;\, C,\gamma,\vartheta)$ of equation (4.7) (regular up to a limiting Mach wave) which for $x,y \to o$ approaches $\varphi_R(x,r;\, C,\gamma)$ and for $r = 1$ satisfies the condition (4.21). Assuming the existence of such a solution for $C = 1$, $\gamma = 0$, and denoting it by $F_R(r,\zeta;\vartheta)$, the general solution is

$$\Phi_R(x,r;\, C,\gamma,\, \varepsilon_1\delta - \tfrac{1}{2}\varepsilon_2\delta^2) \equiv C^{-3} F_R\left[r,\, C(\gamma+1)^{-1/3} x r^{-4/7};\; C^2(\gamma+1)^{-2/3}(\varepsilon_1\delta - \tfrac{1}{2}\varepsilon_2\delta^2)\right] \tag{4.22}$$

The analogous result for plane flow is

$$\Phi_P(X,Y;\, C,\gamma,\, \varepsilon_1\delta^2) \equiv C^{-3} F_P\left[Y,\, C(\gamma+1)^{-1/3} X Y^{-4/5};\; C^2(\gamma+1)^{-2/3}\varepsilon_1\delta\right] \tag{4.23}$$

The limiting values F_P^{∞} and F_R^{∞} as defined by equation (4.17) now become

functions of ϑ, $F_P^\infty(\vartheta)$ and $F_R^\infty(\vartheta)$ say, the equations (4.18), (4.19), and (4.20) remaining valid for $\upsilon = C^2 \varepsilon_1 \delta$ and $\vartheta = C^2(\varepsilon_1\delta - 1/2\varepsilon_2\delta^2)$ respectively, i.e. with

$$\left.\begin{aligned} F_P^\infty &= F_P^\infty\left[C_P^2(\gamma+1)^{-1/2}(\tau c)^{-1/2}\varepsilon_1\delta\left[c\tau^{-1/3}(\gamma+1)^{-1/3}\right]^{1/10}\right] \\ F_R^\infty &= F_R^\infty\left[C_R^2(\gamma+1)^{-1/2}(\tau c)^{-1}(\varepsilon_1\delta - \tfrac{1}{2}\varepsilon_2\delta^2)\left[c\tau^{-1}(\gamma+1)^{-\frac{1}{2}}\right]^{1/7}\right] \end{aligned}\right\} \qquad (4.24)$$

Since experiments (Reference 3) show that M_{ch} increases with the boundary layer thickness it might be conjectured that $-F_P^\infty$ and $-F_R^\infty$ decrease when ϑ increases from zero.

For large models one-dimensional theory gives

$$\left.\begin{aligned} M_{ch} &= 1 - \left(\frac{\gamma+1}{2}\right)^{\frac{1}{2}}(\tau c)^{\frac{1}{2}}\left[1 + \frac{\varepsilon_1^2\delta^2}{2(\gamma+1)c\tau}\right]^{\frac{1}{2}} + \frac{1}{2}\varepsilon_1\delta \\ M_{ch} &= 1 - \left(\frac{\gamma+1}{2}\right)^{\frac{1}{2}}\tau c\left[1 + \frac{2}{\gamma+1}\left(\frac{\varepsilon_1\delta - \frac{1}{2}\varepsilon_2\delta^2}{\tau c}\right)^2\right]^{\frac{1}{2}} + \varepsilon_1\delta - \frac{1}{2}\varepsilon_2\delta^2 \end{aligned}\right\} \qquad (4.25)$$

in two and three dimensions respectively. It is seen that when the boundary layer thickness is so small that only linear terms in δ have to be kept, then the increment in M_{ch} due to the wall boundary layer is independent of the size and form of the model. Furthermore, the same conclusion is valid in the case of small models if only $F_P^\infty(\vartheta)$ and $F_R^\infty(\vartheta)$ are twice differentiable at $\vartheta = 0$, since then we have from equations (4.19), (4.20) and (4.24):

$$\left.\begin{aligned} M_{ch} &= \left[M_{ch}\right]_{\delta=0} + \tfrac{1}{2}F_P^{\infty\prime}(0)\varepsilon_1\delta + O(\delta^2) \\ M_{ch} &= \left[M_{ch}\right]_{\delta=0} + \tfrac{1}{2}F_R^{\infty\prime}(0)\varepsilon_1\delta + O(\delta^2) \end{aligned}\right\} \qquad (4.26)$$

Now this is in qualitative agreement with the experimental results of Petersohn (Reference 3), who explicitely noted that the boundary layer influence on choking Mach number was the same for several models having different values of c and τ [+].

[+] A quantitative comparison between theory and the experiments of Reference 3 is not possible, however, since the values of $\varepsilon_1\delta$ are not known for the boundary layers used, and since humidity effects were believed to be involved

4.4 The correction problem

In the preceding paragraph we have studied the flow at choking under the assumption that the perturbation field at the model approaches that of unbounded sonic flow. We do not know, however, how small the model has to be to justify this assumption. Knowing that, we would solve the correction by choosing the largest model compatible with interpretation of the pressure distribution as belonging to $M_\infty = 1$. The object of the present paragraph is to discuss this choice as influenced by the wall boundary layers.

Suppose that the structure of a field at choking may be described in the following terms. In a region I (see Figure 13) next to the model the perturbation potential is the same - in some reasonable sense - as would be there in unbounded sonic flow, while outside I it may be approximated by a basic solution associated with the boundary layer present. At the wall the potential of course is different from the asymptotic field pertaining to unbounded sonic flow, but it is assumed that the difference is limited to a region II which does not reach the region I. Then there is a region between I and II, where the basic solution for unbounded sonic flow provides a good approximation.

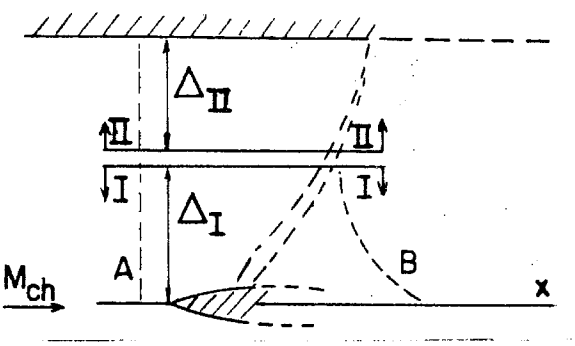

Fig. 13. Structure of flow field at choking

For increasing model size the regions I and II will eventually get into contact with each other. Only contact between those parts of I and II will eventually get into contact with each other. Only contact between those parts of I and II which are situated between the limiting Mach wave and a plane A, located a short distance in front of the model (see Figure 13),

have to be considered. Errors introduced behind the limiting Mach wave cannot propagate upstream of the Mach wave B of Figure 13. In particular, the shock wave system lies completely outside the interference picture (except for very long models). The errors in front of the plane A are of the order of magnitude $1-M_{ch}$, but their influence at the model may be negligible. This is so, since one-dimensional theory should be sufficient for determining a correcting wall deformation, the isobars at A being essentially perpendicular to the x-axis when $1-M_{ch}$ is large.

For still larger models it may be, that there is no zero-interference region at the model, although this cannot a priori be taken for granted. Playing it safe, we shall here not consider larger models than those corresponding to contact between I and II.

Let Δ_I and Δ_{II} be the lateral extensions of the regions I and II, defined in such a way that $\Delta_I + \Delta_{II} = 1$ means contact (see Figure 13). We are then able to estimate from the similarity considerations of the preceding paragraphs how Δ_I and Δ_{II} depend upon the form and size of the model. From equations (4.10) and (4.12) it follows that

$$\Delta_I = \begin{cases} K_P (\gamma+1)^{-1/3} \tau^{-1/3} c \\ K_R (\gamma+1)^{-1/2} \tau^{-1} c \end{cases} \tag{4.27}$$

where the constants of proportionality K_P and K_R, for plane and three-dimensional flow respectively, depend upon the form of the model. The parameter ϑ determines the basic solutions ϕ_P and ϕ_R uniquely, and hence Δ_{II} in the form

$$\Delta_{II} = \begin{cases} h_P \left[c_P^2 (\gamma+1)^{-\frac{1}{2}} (\tau c)^{-\frac{1}{2}} \varepsilon_1 \delta \left[c \tau^{-1/3} (\gamma+1)^{-1/3} \right]^{1/10} \right] \\ h_R \left[c_R^2 (\gamma+1)^{-\frac{1}{2}} (\tau c)^{-1} (\varepsilon_1 \delta - \tfrac{1}{2} \varepsilon_2 \delta^2) \left[c \tau^{-1} (\gamma+1)^{-\frac{1}{2}} \right]^{1/4} \right] \end{cases} \tag{4.28}$$

where the functions $h_p(\vartheta)$ and $h_R(\vartheta)$ apply to plane and circular test sections respectively.

To determine the functions $h_p(\vartheta)$ and $h_R(\vartheta)$ comprehensive computations (or experiments) are required. An overall picture of their form can however be surmised from the following reasoning. Figure 14 shows, how one has to reshape the wall in the critical region between $x = 0$ and the limiting Mach wave to have no interference with the basic potential $\varphi_p(x,y;1,0)$ for unbounded plane flow. The contour with no boundary layer ($\vartheta=0$) coincides of course with the stream line of Figure 10. In the general case the wall deformation $\Delta Y(x)$ is computed by integrating the boundary condition at the wall

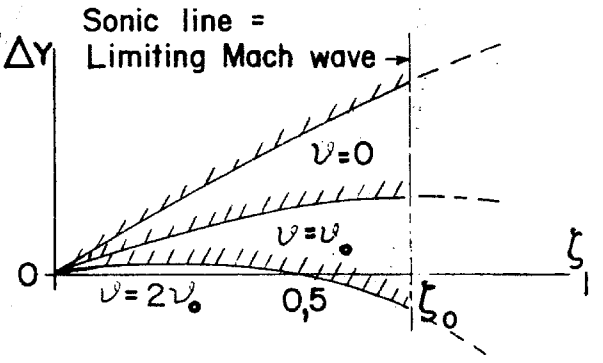

Fig. 14. Wall contours for zero interference

$$y = 1 \quad : \quad \frac{\partial \varphi}{\partial Y} = \frac{d}{dX} \Delta Y + \vartheta \frac{\partial^2 \varphi}{\partial X^2}$$

with respect to x. The contours of Figure 14, obtained in this way, have been normalized to pass through the point $x = 0$, $y = 1$. Since $h_p(\vartheta)$ in a sense measures the wall interference of the undeformed wall on φ_p, one would expect a small value of h_p to correspond to a slightly deformed wall and vice versa. From Figure 10 it is seen that $\frac{\partial^2 \varphi_p}{\partial X^2} > 0$, $\frac{\partial \varphi_p}{\partial Y} > 0$, and hence that a small positive value of ϑ means an everywhere reduced wall deformation as compared to the case $\vartheta = 0$. For specific value $\vartheta = \vartheta_0$ the slope at the sonic line becomes zero (= the slope of the undeformed wall), data from Reference 24 giving $\vartheta_0 = 0.483$. For $0 \leq \vartheta < \vartheta_0$ the slope is everywhere positive. When ϑ increases beyond ϑ_0 the slope becomes nega-

tive, first next to the sonic line only, but then everywhere and with ever increasing magnitude. This behavior indicates h_p to have a minimum at $\mathcal{V} = k_p \cdot \mathcal{V}_o$, where k_p is a positive constant not much different from one.

The three-dimensional case is not essentially differenct. Zero slope at the sonic line is obtained for $\mathcal{V}_o = 0.645$, and $h_R(\mathcal{V})$ is expected have a minimum for $\mathcal{V} = k_R \mathcal{V}_o$ where k_R is close to one.

Recalling equations (4.27) and (4.28) for Δ_I and Δ_{II}, let us consider a model of given form and relative thickness. When the model is very small the region I does not reach the region II, and furthermore a thin boundary layer is sufficient to give Δ_{II} its minimum value. The model growing, Δ_I increases while Δ_{II} still can be kept constant at its minimum by increasing the boundary layer thickness. In practice there is however an upper limit to the boundary layer thickness attainable. Therefore, while increasing the model size until $\Delta_I + \Delta_{II} = 1$, there are two possibilities: either Δ_{II} still has its minimum value, or Δ_{II} has a greater value corresponding to the thickest boundary layer available. In any case the model is larger than would be possible without a boundary layer, the gain in model size being greater in the first case than in second.

If we however make the relative thickness τ smaller, while keeping $\Delta_I + \Delta_{II} = 1$[+], then the optimum boundary layer becomes thinner. Therefore - for a given family of affine models - there is a limit to τ below which the gain in model size is constant but above which the gain decreases with increasing τ.

Up to now terms like small and large have been used without any reference to practical values of model size and relative thickness. It is however possible to make them somewhat more precise. For a particular model

---

[+]Note that this condition requires a reduction of c.

Barish in Reference 22 gives data from which it might be concluded that the constant K_p inequation (4.27) is $K_p \simeq 4$. In Figure 22 what essentially amounts to the optimum boundary layer thickness (for which $v = k_p \cdot v_o$) has been plotted against the thickness of the model, with the relative thickness τ as a parameter. A necessary condition for our considerations to be valid is, that we stay within the region where $\Delta_I < 1$. In Figure 22 this region is situated to the left of a curve $\Delta_I = 1$, and a few such curves have been plotted corresponding to typical values of K_p. It is seen that if the scale factor $C_p^2 \varepsilon_1 K_p^{-1}$ is not much smaller than one - our previous estimates indicating it to be between 1/2 and 1 - then an essential part of the τc-field is covered by reasonable values of the boundary layer thickness.

The corresponding diagram for a circular test section in Figure 23 may permit the same conclusion to be drawn. However, the magnitude of the constant K_R for Δ_I is quite uncertain in this case. Not even for bodies of revolution is there any information available permitting a good estimate.

In conclusion the analysis performed - loose as it may be - indicates that by choosing the thickness of the wall boundary layers in a proper way one should be able to increase the maximum model size for which test results at choking can be interpreted as belonging to unbounded sonic flow. just how large the gain in model size may be is a problem for further investigation.

V. CONCLUSIONS

5.1 Boundary layer problems

Throughout the present study it has been assumed that viscosity can be neglected when establishing a relationship between the displacement effect of the wall boundary layers and the pressure perturbation due to the model. The evidence brought forth for the validity of this basic assumption applies to the case of turbulent boundary layers only. It rests essentially on the fact that the low speed part of the boundary layer next to the wall, where the viscous stress perturbation is bound to be important, is very thin. If we supplement this argument by noting that conclusions derived from the zero-viscosity assumption are reasonable and show qualitative agreement with experimental results, the reason should be only to emphasize that conclusive experimental evidence is not available.

Assuming the undisturbed flow to be cylindrical (i.e. the Mach number to be constant along streamlines) it is possible to define a potential for the perturbation due to the model when within the wall boundary layers. Approximate integration - in the spirit of boundary layer theory - of the differential equation for the perturbation potential in the boundary layer leads to a simple boundary condition for the outer flow, valid if the boundary layer thickness is sufficiently small. This approximate boundary condition expresses the change of mass flow density due to the pressure perturbation and also the redistribution of mass flow due to crossflow within the boundary layer. The condition permits an extension of the transonic similarity rules only if the crossflow is negligible.

The application to linear wall interference theory indicates that boundary layers likely to occur in practice are within the range of validity

of the approximate boundary condition. Moreover, at high subsonic Mach numbers, where the boundary layer influence is large, crossflow seems to stand for a minor contribution only.

The assumption of the undisturbed flow being cylindrical is justified only if the boundary layer thickness is nearly independent of the streamwise coordinate over that part of the wall which contributes most to the interference. Although no attempt has been made to formulate this condition more precisely, the following comment might be relevant. The boundary layer influence is large if the Mach number is close to one, or if the boundary layers are thick, or both. In the first case the critical part of the wall is situated immediately in front of the sonic line approaching or reaching the wall, and it is thought to be comparatively short. In the second case the effective upstream length of the boundary layer is large and therefore the relative change of boundary layer thickness over the critical part of the wall might be small.

A simple and adequate way of checking the applicability of the approximations adapted might be to investigate in some detail the boundary layer perturbation at choking for a typical test body. The case of rotational symmetry should provide a clean experimental setup. If a satisfactory correlation is established between the theoretical and experimental values of the choking Mach number M_{ch}, it might then be possible to adapt measurement of M_{ch} as a routine method for determining the "effective" boundary layer thickness $\varepsilon_1 \delta$ in any test section (instead of measuring at several positions the Mach number distribution of the wall boundary layers).

Only little information having been given earlier in this study on the properties of wall boundary layers occurring in practice, a brief

comment might be appropriate here. The decisive factor for the relative thickness of a natural turbulent boundary layer is the ratio of upstream length to the lateral extension of the test section, current differences in Reynolds number being only of minor importance. Taking the semi-height of the test-section as the unit of length one finds the thickness likely to have a value between 1/20 and 1/10. To obtain thicker boundary layers some disturbing device has to be introduced in the upstream part of the boundary layer (see References 3 and 35). It is to be required from the device that the boundary layer produced has a very thin low-speed wall layer and an almost constant value of $\varepsilon_1 \delta$ over the critical part of the wall, that the streamlines in the boundary layer are parallel to the test section, and that the flow in the test section is steady and uniform. It seems conservative to assume that one can design such a device to increase $\varepsilon_1 \delta$ by at least a factor of two. However, for a given tunnel the upper limit for $\varepsilon_1 \delta$ may be set by the power available, since the pressure losses of the tunnel flow are bound to increase with the boundary layer thickness. A careful redesign of the diffuser for minimum pressure loss may be necessary to reach reasonably high values of $\varepsilon_1 \delta$ and M_o.

5.2 Interference problems

In the Introduction two fundamental problems were formulated to be the subject of any study of the influence of wall boundary layers in transonic test sections, and it is thought proper to repeat them at this point:

I. To what extent is the influence appreciable for those boundary layers which exist in current tunnels, and how can corrections be determined?

II. Is it possible to choose the wall boundary layers to give a considerable reduction of the wall interference, and how can the proper choice be accomplished?

As far as linear theory is applicable for the determination of wall corrections, the results of Chapter III should provide the answers to both questions. With the exception of lift corrections in three-dimensional flow all corrections were found to decrease rapidly with increasing boundary layer thickness for the free-stream Mach number M_o approaching one. As typical figures may be quoted that the boundary layer thickness found necessary for reducing the corrections by half is of the order 1/5 (the semi-height of the test section having unit length) at $M_o = 0.85$, and of the order 1/10 at $M_o = 0.93$.

Let us begin with Problem I. Since natural wall boundary layers usually will be slightly thinner than 1/10, the boundary layer influence on the corrections thus is likely to be relatively large only at Mach numbers greater than $M_o = 0.9$. However, although it should not be difficult to specify conditions under which accurate knowledge of the linear corrections for the boundary layer influence is important, the situation might in many cases be as follows. To make certain that useful data are obtained at the highest Mach numbers to be tested, the model is chosen so small that linear correction theory for zero boundary layer thickness still is valid. At those high Mach numbers where the relative contribution from the boundary layers is large this means very small models, and the corrections might then be so small - compared to the accuracy of the measurements - that they are negligible.

Now, the situation described calls for the following comment, which may well contain the final answer to Problem I. As was noted in Section 3.5 the wall boundary layers do not only work to decrease the corrections but also to extend the zero-interference region at the model, thus permitting larger models to be used. In fact, the results indicate that the bound-

ary layer thickness giving the largest zero-interference region is approximately the same as that reducing the corrections by half. If advantage is taken of this fact by choosing a larger model, one may arrive at a situation where the corrections for the influence of the wall boundary layers are no longer negligible.

The comment just given may also contain an answer to Problem II as far as linear correction theory is concerned. When choosing the boundary layer thickness to minimize the wall interference for a given model one should try to reach as high a value as possible for the corrected Mach number M_∞ without violating the conditions for linear theory to be applicable. It seems reasonable to assume that the optimum thickness is approached by increasing M_o until the limit for linear theory is reached while adjusting simultaneously the thickness to make the region of zero interference as large as possible. The data of Section 3.5 indicate that for $M_o > 0.85$ the optimum thickness for a natural boundary layer is not greater than 1/5. How much M_∞ can be increased for a given model by a proper choice of the boundary layer thickness (or how much the size of the model can be increased for a given maximum of M_∞) is a problem for experimential investigation.

Leaving linear theory we have material for a discussion of Problem II only in the case of choked flow. In Chapter IV the application of similarity considerations to the basic sonic solutions of Guderley et al. made it possible to formulate vague conditions for the choked flow at the model to be interpreted as corresponding to unbounded sonic flow ($M_\infty = 1$). The analysis indicates that the maximum model size permitting this interpretation might be increased by choosing the thickness of the wall boundary

layers properly, although no conclusion can be drawn as to the gain made possible. Furthermore, the optimum thickness seems to be well within the region of practically available boundary layers. It is only in the case of plane flow, however, that it has been made probable that the results obtained apply to models of reasonable size, the three-dimensional analysis possible applying only to very small models. A somewhat more refined approach, involving small perturbation analysis of the basic potential along the lines followed by Guderley in Reference 21, may prove useful. In any case, considerable experimental work will be required to make possible an optimum choice of model size and wall boundary layer thickness at choking.

The attitude taken in defining the optimum wall boundary layer in the sense of Problem II in the case where linear correction theory is applicable as well as in the case of choking may be described as the principle of minimizing interference rather than corrections. If an experimental investigation of the choking case proves successful the next step would be to look into the range of intermediate Mach numbers where no reasonably simple theory is available. One would the, following the principle stated, try to establish criteria for the model size and the boundary layer thickness, which would ensure that to a given unbounded flow field of Mach number M_∞ there always corresponds a tunnel flow field with approximately the same pressure distribution at the model. Still in accordance with our principle we could then be perfectly satisfied to know that in the intermediate range the mapping between the two families of fields is one-one, the actual magnitude of the corrections being of no greater importance since they are limited to the narrow range determined by the known corrections at the endpoints of the intermediate range.

To conclude this discussion of interference problems, it should be

noted that although the quantitative analysis of the present study has been applied to plane and circular test sections only, there is reason to believe the results for the circular test section to be qualitatively valid also for other three-dimensional test sections. This is so, since at transonic speeds the perturbations decay only slightly in transversal directions, this fact constituting an averaging process of the perturbations over the cross section of the tunnel[+]. Finally, the linear theory of Chapter III can easily be extended to provide precise information for rectangular test sections (an approximate analysis of the boundary layer flow in the corners may be necessary).

5.3 Outlook

In the preceding paragraph we have discussed problems associated with the use of thick wall boundary layers in closed test sections as a means of increasing the largest model size permitting tests in the complete range of subsonic Mach numbers (including choking). The problems were seen to be both many and complicated, and thus the following question arises in a natural and unavoidable way. Would it not - for the purpose specified - be simpler to use the modern technique of slotted walls (on which data recently have been made public), thus, in addition, getting the possibility of performing tests at low supersonic Mach numbers? In the opinion of the present author the answer will in most cases be in the affirmative, although under special circumstances, as for example where an existing wind tunnel does not provide sufficient space for a redesigned test section, it could have been preferable to use thick boundary layers. Therefore many of the problems just discussed may not be worth while being pursued any further.

[+] In Section 4.2 essentially the same argument was used to extend results for bodies of revolution to arbitrary slender bodies.

However, even when using a slotted test section, the influence of the wall boundary layers may be important. One would for example expect that the slot area to be used depends upon the thickness of boundary layers present. When using halfmodels the boundary layer at the reflection plate might cause trouble at transonic Mach numbers. When making tests with oscillating models in closed tunnels the wall interference may become very large even for low frequencies if the Mach number is close to one (see References 31 and 32), and it seems likely that in a slotted test section the same phenomenon of resonance may occur even when the interference at steady flow is negligible. If this is the case the wall boundary layers are likely to form an important part of the interference picture.

The examples cited define problems that should be investigated experimentally. They do also define theoretical problems which could be treated by methods similar to those developed in the present paper.

REFERENCES

1. Millikan, C.B., Smith, J. E., and Bell, R.W., High-speed testing in the Southern California Cooperative Wind Tunnel, J. Aeron. Sci. 15, 69 (1948).

2. Evans, J.Y.G., Corrections to velocity for wall constraint in any 10 x 7 rectangular subsonic wind tunnel, A.R.C. R and M. 2662 (1949).

3. Petersohn, E.G.M., Some experimental investigations on the influence of wall boundary layers upon wind tunnel measurements at high subsonic speeds, Aeron. Res. Inst. of Sweden (FFA), Rep. 44 (1952).

4. Oswatitsch, K., and Wieghardt, K., Theoretische Untersuchungen über stationäre Potentialströmungen und Grenzschichten bei hohen Geschwindigkeiten, Lilienthal-Gesellschaft für Luftfahrtforschung Bericht S 13/1, 7 (1943), reprinted as NACA TM 1189.

5. Ackeret, J., and Rott, N., Ueber die Stömung van Gasen durch ungestaffelte Profilgitter, Schweiz. Bauzeitung 67, 40 (1949).

6. Lighthill, M.J., On boundary layers and upstream influence, II. Supersonic flows without separation, Proc. Roy. Soc. A, 217, 478 (1953).

7. Berndt, S.B., On the theory of weak steady disturbances to boundary layers (in Swedish)., Aeron. Res. Inst. of Sweden, Rep. AE-217 (1953).

8. Tsien, H.S., and Finston, M., Interaction between parallel streams of subsonic and supersonic velocities, J. Aeron. Sci., 16, 515 (1949).

9. Berndt, S.B., Approximate calculation of the influence of wall boundary layers upon the blockage interference in a high speed wind tunnel, Aeron. Res. Inst. of Sweden (FFA), Rep. 45 (1952).

10. Vandrey, F., Die Reflexion Schwacher Störungen and Unsstetigkeitsflächen einer ebenen Unterschallströmung, Z. ang. Math. Mech. 29, 1 (1949).

11. Chuan, R.L., A heat cycle low Reynolds number transonic tunnel, J. Aeron. Sci. 20, 59 (1953).

12. Courant, R., and Hilbert, D., Methoden der Mathematischen Physik, II, Berlin (1937).

13. Ackeret, J., Degen, M., and Rott, N., Ueber die Druckverteilung an schräg angeströmten Rotationskorpern bei Unterschallgeschwindigkeit, Aerotecnica 31, 11 (1951).

14. Lighthill, M.J., Reflection at a laminar boundary layer of a weak steady disturbance to a supersonic stream, neglecting viscosity and heat conduction, Qu. J. Mech. and Appl. Math. 3, 303 (1950).

15. Spreiter, J.R., On the application of transonic similarity rules, NACA TN 2726 (1952).

16. Spreiter, J.R., and Alksne, A., Theoretical prediction of pressure distributions on non-lifting airfoils at high subsonic speeds, NACA TN 3096 (1954).

17. Lin, C., Reissner, E., and Tsien, H.S., On two-dimensional nonsteady motion of a slender body in a compressible fluid, J. Math. and Physics 27, 220 (1948).

18. Hayes, W.D., The three-dimensional boundary layer, NAVORD Rep. 1313 (1951).

19. Taylor, G.I., Strömung un einen Körper in einer kompressiblen Flüssigkeit, Z. ang. Math. Mech. 10, 334 (1930).

20. Guderley, G., and Yoshihara, H., An axial-symmetric transonic flow pattern, Q. Appl. Math. 8, 333 (1951).

21. Guderley, G., Axial-symmetric flow patterns at a free stream Mach number close to one, USAF TR 6285 (1950).

22. Barish, D.T., Interim report on a study of Mach one wind tunnels, USAF WADC TR 52-88 (1952).

23. Guderley, G., Singularities at the sonic velocity, USAF F-TR-1171-ND (1948)

24. Barish, D.T., and Guderley, G., Asymptotic forms of shock waves in flows over symmetrical bodies at Mach 1, J. Aeron. Sci. 20, 491 (1953).

25. Guderley, G., and Yoshihara, H., Axial-symmetric flow patterns, USAF TR 5797 (1949).

26. Guderley, G., and Yoshihara, H., Two-dimensional unsymmetric flow pattens at Mach number 1, J. Aeron. Sci. 20, 757 (1953).

27. Berndt, S.B., Wind tunnel interference due to lift for delta wings of small aspect ratio, Roy. Inst. Tech. Stockholm, KTH Aero. TN 19 (1950).

28. von Kármán, Th., The similarity law of transonic flow, J. Math. and Physics 26, 182 (1947).

29. Oswatitsch, K., Die Theoretische Arbeiten über schallnahe Strömung am Flugtechnischen Institut der Königl. Technischen Hochschule, Stockholm, paper read at 8th Internat. Appl. Mech. Congress in Istanboul (1952).

30. Keune, F., and Oswatitsch, K., Nicht angestellte Körper kleiner Spannweite in Unter- und Ueberschallströmung, Z. für Flugwissenschaften 1, 137 (1953).

31. Runyan, H. L. and Watkins, Ch.E., Considerations on the effect of wind-tunnel walls on oscillating air forces for two-dimensional subsonic compressible flow, NACA TN 2552 (1951).

32. Woolston, D.S. and Runyan, H.L., Some considerations on the air forces on a wing oscillating between two walls for subsonic compressible flow, Inst. Aeron. Sci. Reprint 446 (1954).

33. Liepmann, H.W., Askenas, H. and Cole, J.D., Experiments in transonic flow, USAF TR 5667 (1948).

34. Liepmann, H.W., Roshko, A. and Dhawan, S., On reflection of shock waves from boundary layers, NACA Rep. 1100 (1949).

35. Klebanoff, P.S. and Diehl, Z. W., Some features of artificially thickened fully developed turbulent boundary layers with zero pressure gradient, NACA Rep. 1110 (1950).

APPENDIX A. LIST OF SYMBOLS

a	local speed of sound; equation (2.3)
c	characteristic model length in streamwise direction; Figures 6 and 11
C	parameter of basic solutions; equation (4.9)
$C(k)$	equations (3.17) and (3.32)
C_P, C_R	form parameters of models; equations (4.11) and (4.13)
$\frac{D}{D\zeta}$	derivative with respect to position of zero-interference point; equation (3.14)
e_1, e_2	form parameters for jet boundary layer; equation (2.28)
f^{mn}	odd and even parts of wall pressure distribution; equations (3.18) and (3.33)
f_P, f_R	equations (4.5) and (4.8)
F^{mn}	Fourier kernels for f^{mn}; equations (3.19) and (3.34)
F_P, F_R	equations (4.15) and (4.16); superscript ∞ indicates upstream values as defined in equation (4.17)
g^{mn}	odd and even parts of φ_∞; equations (3.8) and (3.24)
G^{mn}	Fourier kernels for g^{mn}; equations (3.15) and (3.30)
G_o, G_1, G'	Regions of undisturbed flow in test section: Figure 1
h^{mn}	odd and even parts of φ_w; equations (3.10) and (3.25)
$h_P(\nu)$, $h_R(\nu)$	equation (4.28)
k	wave number in Fourier transform with respect to x; equation (3.15)
k_P, k_R	coefficients for optimum boundary layer thickness at choking
K_P, K_R	coefficients for Δ_I
m	$= 3n-2$
$m(\nu)$	$= \frac{M}{M_o}$
$M(y,z)$, M_o	Mach number of tunnel flow; Figure 1
M_∞	Mach number of unbounded flow

M_{ch}	choking Mach number
$\frac{\partial}{\partial n}$	derivative in direction of inward normal
n	= 4/5 for plane flow, and = 4/7 for three-dimensional flow; equations (4.4) and (4.8)
p	pressure of perturbed flow
P	pressure of undisturbed flow
r	radius perpendicular to x-axis; Figure 5
R	$= \xi^2 + y^2$ or $= \xi^2 + r^2$
R	radial coordinate of streamline far upstream
R(y,z)	density of air in undisturbed flow
s	arc length on Γ_1; Figure 2
S(k)	equations (3.17) and (3.32)
u,v,w	components of perturbation velocity; equation (2.2)
U(y,z)	velocity of undisturbed flow; equation (2.1)
x,y,z	Cartesian coordinates; Figure 1
Y,Z	upstream coordinate of streamline
α_o, α_∞	angle of attack of model in test section and in unbounded flow respectively
δ	thickness of wall boundary layer
ΔM_o, $\Delta\alpha_o$	wall corrections; equation (3.1)
Δ I, Δ II	lateral extension of regions I and II as shown in Figure 13
ε_1, ε_2	form parameters for wall boundary layer; equation (2.4)
γ	ratio of specific heats; equation (2.1)
Γ, Γ_o, Γ_1	cylindrical surfaces bounding test section; Figure 1
ζ	equations (4.4) and (4.8); subscript o indicates sonic line
ϑ	$= c^2\varepsilon_1\delta$ or $= c^2(\varepsilon_1\delta - 1/2\,\varepsilon_2\delta^2)$; subscript o indicates value giving deformed wall of zero slope at sonic line; Figure 14.
$\varkappa$	curvature of Γ_1; equation (2.15)

ν coordinate normal to boundary with δ as unit of length; Figure 2

ξ $= x\sqrt{1 - M_o^2}$

ϱ density of air in perturbed flow; equation (2.2)

τ relative thickness of model; Figure 11

$\varphi(x,y,z)$, $\varphi(x,r,e)$ perturbation potentials; equation (2.7); subscripts ∞, o and w as defined in equation (3.2)

$\varphi(x,\nu,s)$, $\bar{\varphi}(x,\nu,s)$ perturbation potentials; equations (2.17), (2.19) and (2.20)

φ_P, φ_R basic perturbation potentials in unbounded, sonic flow; equations (4.5), (4.8) and (4.9)

Φ_P, Φ_R basic perturbation potentials at choking; equations (4.15) and (4.16)

APPENDIX B. UNIQUENESS THEOREMS

The application of the approximate boundary condition for a thin wall boundary layer to the linear subsonic flow problems of Chapter III raises the question of uniqueness of the solutions found. Two simple uniqueness theorems will therefore be given, one for plane flow and another for the flow in a circular test section.

The following terminology will be used in the case of plane flow. In Euclidean space with Cartesian coordinates xy there is an open rectangular region G. The four sides, making up the boundary Γ of G, are parallel to the axes, the two sides parallel to the x-axis being denoted by Γ_ℓ and Γ_u with $y_u > y_\ell$ (see figure), the two others by Γ_- and Γ_+.

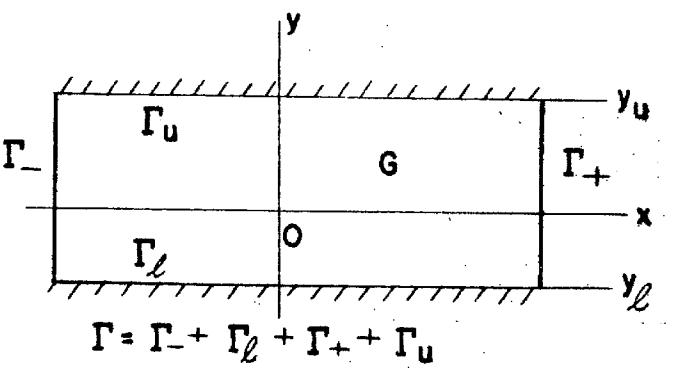

By H^2 we denote the class of functions which are harmonic in G and Twice continuously differentiable in $G + \Gamma$.

Theorem I : If $\varphi(x,y)$ belongs to the class H^2 and satisfies the following boundary conditions:

(i) $\varphi_x = 0$ on Γ_- and Γ_+

(ii) $\varphi_y = - A_\ell \varphi_{xx}$ on Γ_ℓ

(iii) $\varphi_y = A_u \varphi_{xx}$ on Γ_u

where A_ℓ and A_u are non-negative constants, then φ is a constant in G.

Proof: The following identity is valid in G

$$\varphi_{xx}^2 + \varphi_{xy}^2 = \frac{\partial}{\partial x}(\varphi_y \varphi_{xy}) - \frac{\partial}{\partial y}(\varphi_y \varphi_{xx}) + \varphi_{xx}(\varphi_{xx} + \varphi_{yy})$$

if φ has continuous third-order derivatives, as is the case for φ belonging to H^2 (the last term then dropping out). If φ also satisfies the conditions (i), (ii) and (iii) integration over G gives:

$$\iint_G (\varphi_{xx}^2 + \varphi_{xY}^2)\, dx\, dY = -A_\ell \int_{\Gamma_\ell} \varphi_{xx}^2\, dx - A_u \int_{\Gamma_u} \varphi_{xx}^2\, dx$$

Since $A_\ell \geq 0$, $A_u \geq 0$ this is possible only if $\varphi_{xx} = \varphi_{yy} = 0$ in G, i.e. if φ is a linear function of x and y. The boundary conditions permit φ to be a constant only, and thus the proof is complete.

For the circular test section we consider in three-dimensional Euclidean space an open region G bounded by a surface of revolution Γ, consisting of a part Γ_w of a circular cylinder and of two plane surfaces Γ_- and Γ_+ (see figure) perpendicular to the generators of the cylinder. Introducing cylindrical coordinates x,y,θ with the x-axis coinciding with the axis of symmetry of Γ_w, we consider the class H^2 of functions $\varphi(x,r,\theta)$ which are harmonic in G and twice continuously differentiable in $G + \Gamma$ (in the sense of the Euclidean metric). We then have the following theorem.

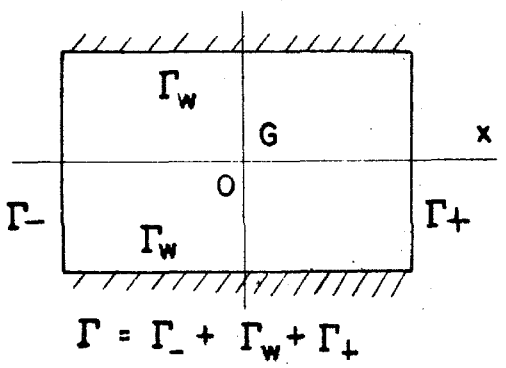

Theorem II : If $\varphi(x,r,\theta)$ belongs to the class H^2 and satisfies the following boundary conditions

(i) $\varphi_x = 0$ on Γ_- and Γ_+

(ii) $\varphi_r = A\varphi_{xx} + B\varphi_{\theta\theta}$ on Γ_w, A and B being non-negative constants,

then φ is a constant in G.

Proof: For $A = B = 0$ the theorem is well known; it expresses the fact that a harmonic function in G with zero normal derivative at Γ is a constant.

We may therefore assume that $A + B > 0$. Integration of the following identity

$$A(\varphi_{xx}^2 + \varphi_{xr}^2 + \frac{1}{r^2}\varphi_{x\theta}^2) + B(\varphi_{x\theta}^2 + \varphi_{r\theta}^2 + \frac{1}{r^2}\varphi_{\theta\theta}^2) =$$

$$= \frac{\partial}{\partial x}\left[A(\varphi_r\varphi_{xr} - \frac{1}{r^2}\varphi_x\varphi_{\theta\theta}) + B\varphi_\theta\varphi_{x\theta}\right] - \frac{1}{r}\frac{\partial}{\partial r}\left[r\varphi_r(A\varphi_{xx} + B\varphi_{\theta\theta})\right] +$$

$$+ \frac{1}{r}\frac{\partial}{\partial\theta}\left[\frac{A}{r}\varphi_x\varphi_{x\theta} + Br(\varphi_r\varphi_{r\theta} - \varphi_\theta\varphi_{xx})\right] + (A\varphi_{xx} + B\varphi_{\theta\theta})(\varphi_{xx} + \varphi_{rr} + \frac{1}{r}\varphi_r + \frac{1}{r^2}\varphi_{\theta\theta})$$

over G gives for φ satisfying the requirements of the theorem the following result:

$$\iiint_G \left[A(\varphi_{xx}^2 + \varphi_{xr}^2 + \frac{1}{r^2}\varphi_{x\theta}^2) + B(\varphi_{x\theta}^2 + \varphi_{r\theta}^2 + \frac{1}{r^2}\varphi_{\theta\theta}^2)\right] r\,dx\,dr\,d\theta =$$

$$= -\iint_{\Gamma_w} \varphi_r^2\, r\,dx\,d\theta$$

For $A > 0$, $B = 0$ this is possible only if φ has the form $\varphi = Dx + f(r,\theta)$. But conditions (i) and (ii) then require D to be zero and f to be a constant (since it is a harmonic function in G with zero normal derivative on Γ).

For $A = 0$, $B > 0$, φ must be of the form $\varphi = E\theta + f(x,r)$. For φ to be regular at the axis E has to be zero, and furthermore f, having zero normal derivative at Γ, has to be a constant.

Finally, for $A > 0$, $B > 0$, φ takes the form $\varphi = Dx + E\theta + f(r)$, and the same arguments as above require D and E to be zero and f to be a constant. This completes the proof.

The theorems given apply to test sections of finite length. To extend them to the case of infinite length one has to restrict oneself to harmonic functions having square-integrable second derivatives in $G + \Gamma$.

APPENDIX C. AN APPROXIMATE BOUNDARY CONDITION FOR SUPERSONIC FLOW

The approximate boundary condition of equation (2.23), expressing the influence of a thin wall boundary layer on the outer flow, is not convenient when the free-stream Mach number M_o is supersonic (see for example Reference 33). One would rather have a condition where the coefficient of $\bar{\phi}_{xx}$ is non-negative and the coefficient of $\bar{\phi}_{ss}$ still is negative. It is possible to achieve this if M_o is sufficiently large by a slightly changed application of the technique of paragraph 2.5. As a matter of fact the coefficient of $\bar{\phi}_{xx}$ can be made zero.

The physical background of this application is roughly the following. A positive Mach number perturbation means that the mass flow density is increased in the subsonic part of the boundary layer and decreased in the supersonic part of the boundary layer. If the supersonic part is thick enough these contributions might cancel, thus leaving only a small net contribution due to change of mass flow density in boundary layer.

We obtained the subsonic boundary condition by substituting for the perturbation potential $\phi(x, \nu, s)$ within the boundary layer a potential $\bar{\phi}$, which is an approximate continuation up to the wall of the potential outside the boundary layer by means of the differential equation (2.18) valid there. In the present case the continuation will not be carried as far as the wall but only up to a cylindrical surface within the boundary layer.

Let this surface be given in the form

$$\nu = \bar{\nu}(s) \quad ; \qquad 0 \le \bar{\nu} \le 1 \tag{C.1}$$

Integration with respect to ν between $\nu = 0$ and $\nu = \bar{\nu}$ of the differential equation (2.16) for ϕ gives

$$\nu = \bar{\nu}: \quad \frac{1-\nu\delta K}{m^2}\frac{\partial\phi}{\partial n} = -\frac{\partial^2\phi}{\partial x^2}\delta\int_0^{\bar{\nu}}(1-\nu\delta K)\frac{1-m^2M_o^2}{m^2}d\nu - \frac{\partial}{\partial s}\left[\frac{\partial\phi}{\partial s}\delta\int_0^{\bar{\nu}}(1+\nu\delta K)\frac{d\nu}{m^2}\right]+O(\delta^3) \tag{C.2}$$

the non-linear transonic term being dropped. Integration of the equation (2.22) for $\bar{\phi}$ between $\nu = \bar{\nu}$ and $\nu = 1$ similarly gives:

$$\nu = \bar{\nu}: \quad (1-\nu\delta K)\frac{\partial \bar{\phi}}{\partial n} = \frac{1-\nu\delta K}{m^2}\frac{\partial \phi}{\partial n} - \frac{\partial^2 \bar{\phi}}{\partial x^2}\delta\int_{\bar{\nu}}^{1}(1-\nu\delta K)\frac{1-m^2}{m^2}d\nu - \\ - \frac{\partial}{\partial s}\left[\frac{\partial \bar{\phi}}{\partial s}\delta\int_{\bar{\nu}}^{1}(1+\nu\delta K)\frac{1-m^2}{m^2}d\nu\right] + O(\delta^3) \tag{C.3}$$

Combining this with equation (C.2) and using the estimate $\phi - \bar{\phi} = O(\delta^2)$ one obtains

$$\nu = \bar{\nu}: \quad (1-\nu\delta K)\frac{\partial \bar{\phi}}{\partial n} = -\frac{\partial^2 \bar{\phi}}{\partial x^2}\delta\left[\varepsilon_1 - \tfrac{1}{2}\delta K\varepsilon_2 - (M_0^2-1)(\nu - \tfrac{1}{2}\delta K\nu^2)\right] - \\ - \frac{\partial}{\partial s}\left\{\frac{\partial \bar{\phi}}{\partial s}\delta\left[\varepsilon_1 + \tfrac{1}{2}\delta K\varepsilon_2 + \nu + \tfrac{1}{2}\delta K\nu^2\right]\right\} + o(\delta^3) \tag{C.4}$$

It is seen that for M_0 sufficiently large the coefficient of $\bar{\phi}_{xx}$ will be positive for $\bar{\nu} \leq 1$. The simplest choice of $\bar{\nu}$, is the one making the coefficient zero:

$$\bar{\nu} = \frac{\varepsilon_1}{M_0^2-1} + \frac{1}{2}\frac{\delta K}{M_0^2-1}\left(\frac{\varepsilon_1^2}{M_0^2-1} - \varepsilon_2\right); \quad 0 \leq \bar{\nu} \leq 1 \tag{C.5}$$

For the values $\varepsilon_1 = 1/2$, $\varepsilon_2 = 1/5$ and $K = 0$ this choice is seen to be possible for $M_0 \geq \sqrt{1.5} \simeq 1.23$. The wall curvature term is zero for $M_0 = 1.5$.

Introduction of $\bar{\nu}$ so determined into equation (C.4) gives:

$$\nu = \bar{\nu}: \quad \frac{\partial \phi}{\partial n} = -\frac{1}{M_0^2-1}\left\{\frac{\partial}{\partial s}\left[\frac{\partial \phi}{\partial s}\left(M_0^2\varepsilon_1\delta + \frac{K\varepsilon_1^2\delta^2}{M_0^2-1} + \frac{M_0^2-2}{2}K\varepsilon\delta^2\right)\right] + \right. \\ \left. + K\varepsilon_1\delta\frac{\partial}{\partial s}\left(\frac{\partial \bar{\phi}}{\partial s}M_0^2\varepsilon_1\delta\right)\right\} + O(\delta^3) \tag{C.6}$$

This expression then, is proposed to be taken as a boundary condition for the perturbation potential of the supersonic outer flow, the potential satisfying a differential equation with constant coefficients ($M = M_0$) up to the cylindrical surface $\nu = \bar{\nu}$. As it stands the condition looks rather complicated, but in the practically important case of negligible δ^2-terms it takes the

following much simpler form

$$\nu = \bar{\nu}: \quad \frac{\partial \phi}{\partial n} = -\varepsilon_1 \delta \frac{M_0^2}{M_0^2-1} \left(\frac{\partial^2}{\partial s^2} + \frac{\delta'}{\delta} \frac{\partial}{\partial s} \right) \bar{\phi} \tag{C.7}$$

Since $0 \leq \bar{\nu} \leq \nu$, one is led to the conclusion that, except for cross-flow effects, the influence of turbulent wall boundary layers on a supersonic outer flow is not large, unless the Mach number is close to one. It should be noted, however, that according to the basic assumptions introduced, the approximate boundary condition is valid only if the thickness δ - without being too small compared to the streamwise length of the perturbed region- is small compared to the small-scale length of the pressure gradient. For example, it can not be applied in case of shock waves reaching the boundary layer, although in this case experiments indicate the qualitative conclusion of small influence to be valid for weak shocks (Reference 34).

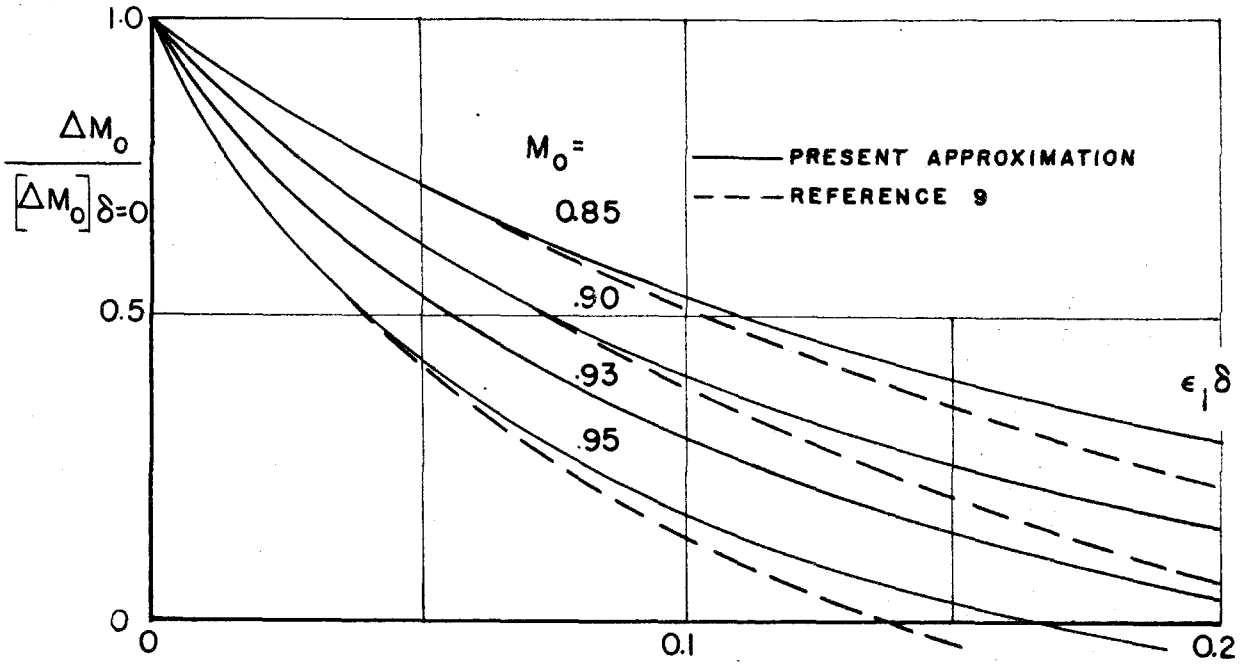

Figure 15. Boundary layer influence on blockage correction for a body in plane flow (linear theory, c = 1/4).

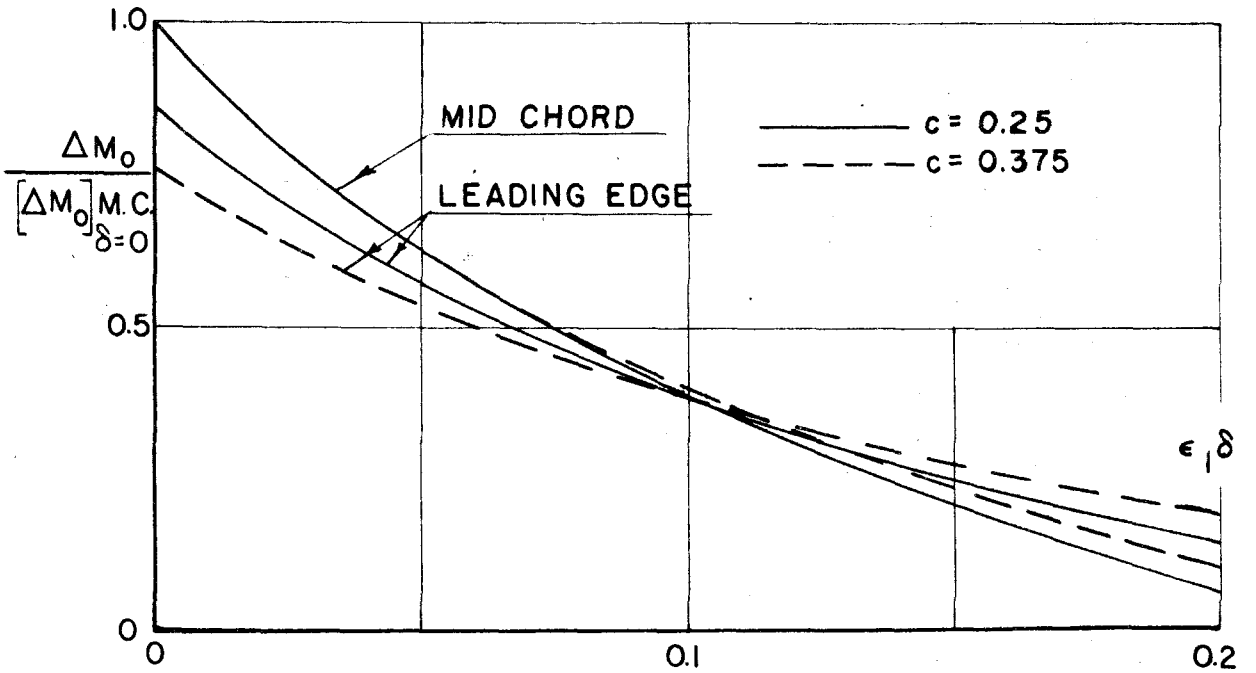

Figure 16. Boundary layer influence on blockage corrections at two different representative points for two different finite bodies (c = 0.25 and 0.375) in plane flow (linear theory).

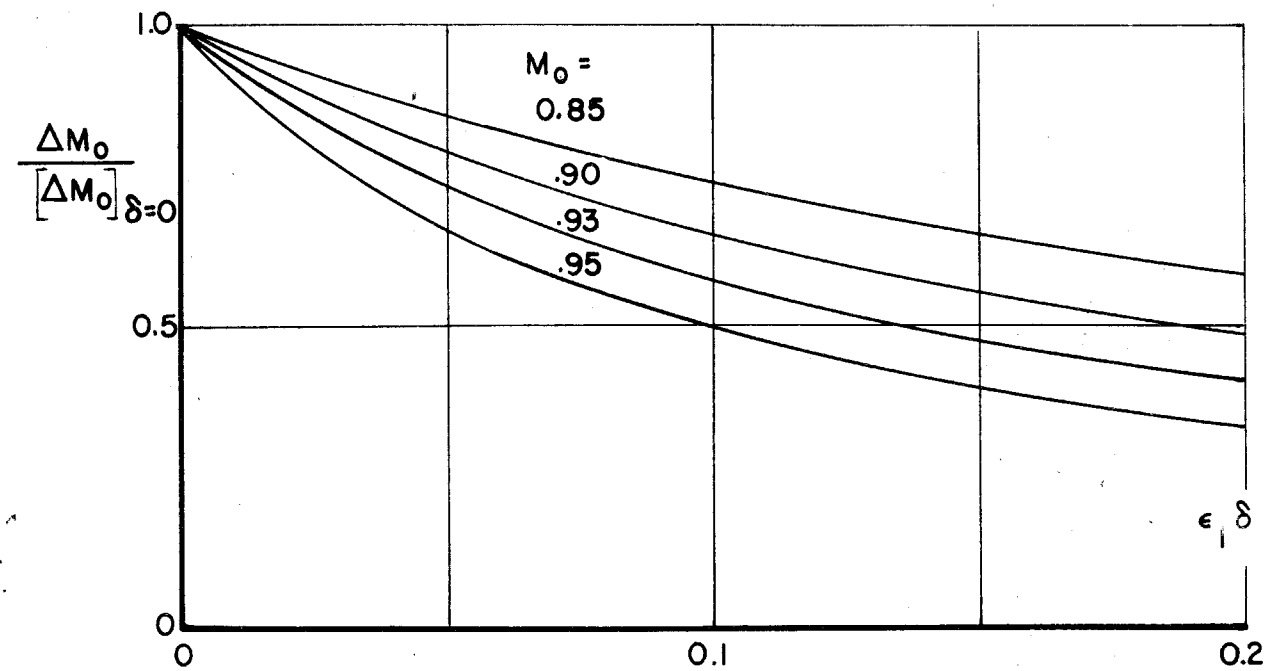

Figure 17. Boundary layer influence on blockage correction for halfbody in plane flow (linear theory).

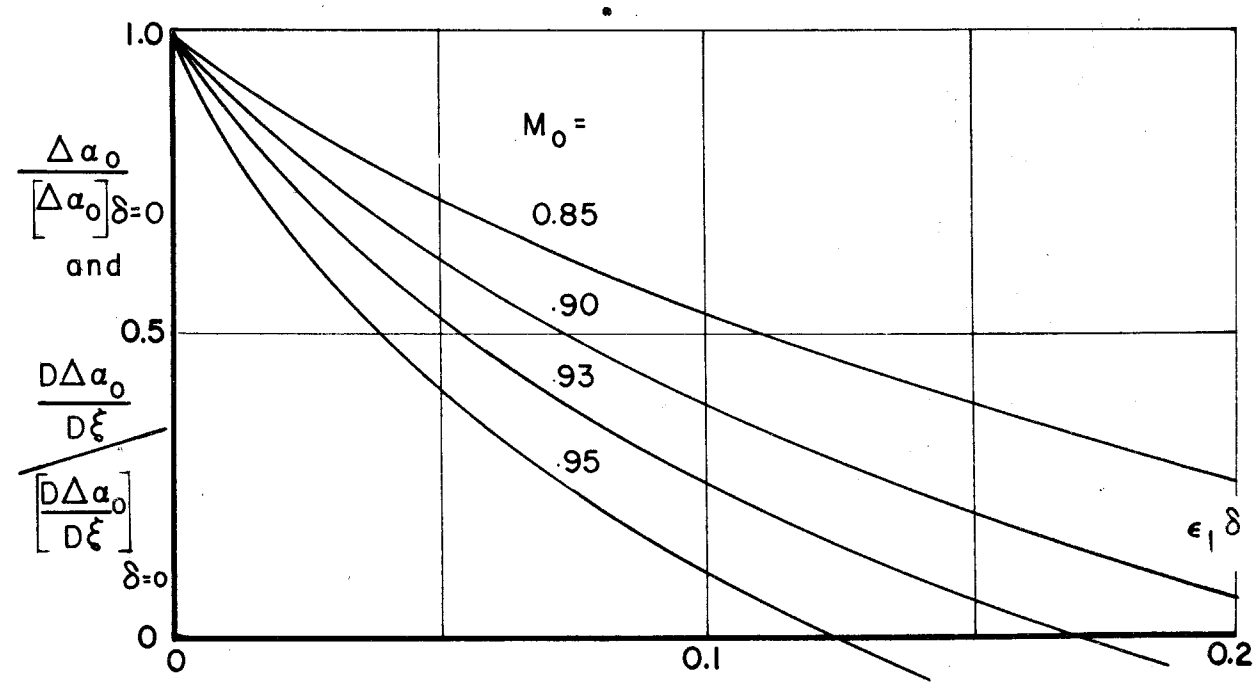

Figure 18. Boundary layer influence on angle-of-attack corrections in plane flow (linear theory, c = 1/4).

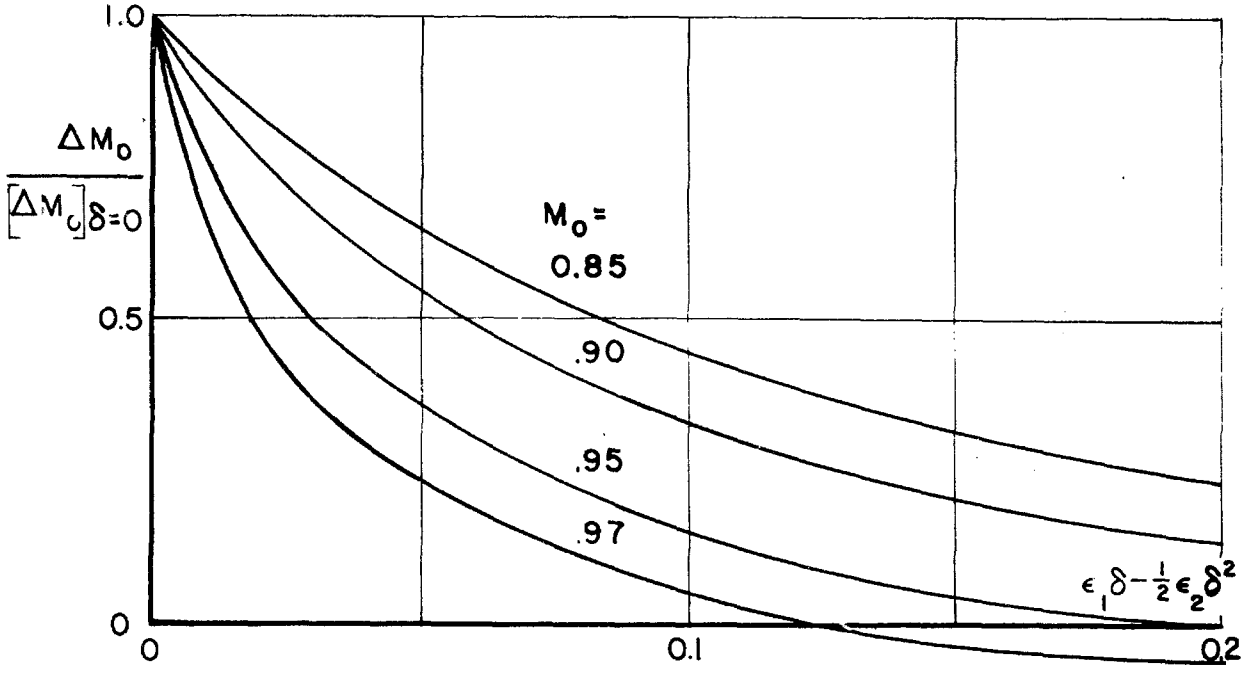

Figure 19. Boundary layer influence on blockage correction for finite body in circular test section (linear theory, c = 0.4).

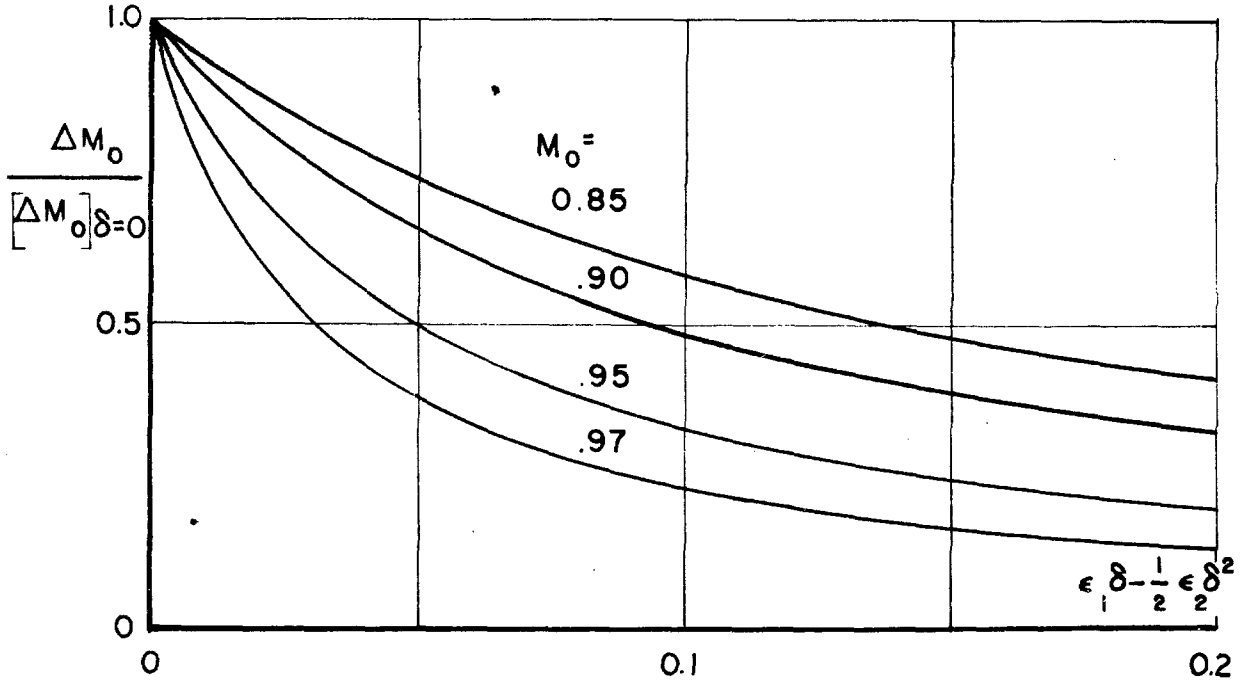

Figure 20. Boundary layer influence on blockage correction for halfbody in circular test section (linear theory).

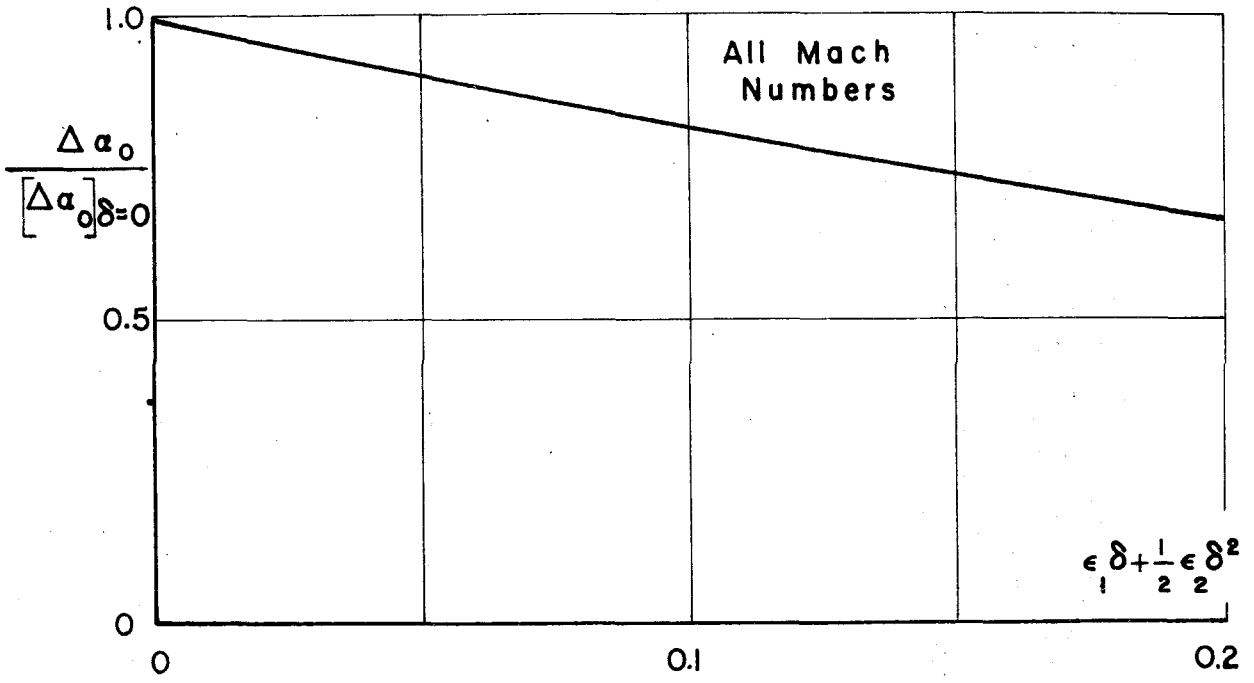

Figure 21. Boundary layer influence on angle-of-attack correction in circular test section (linear theory).

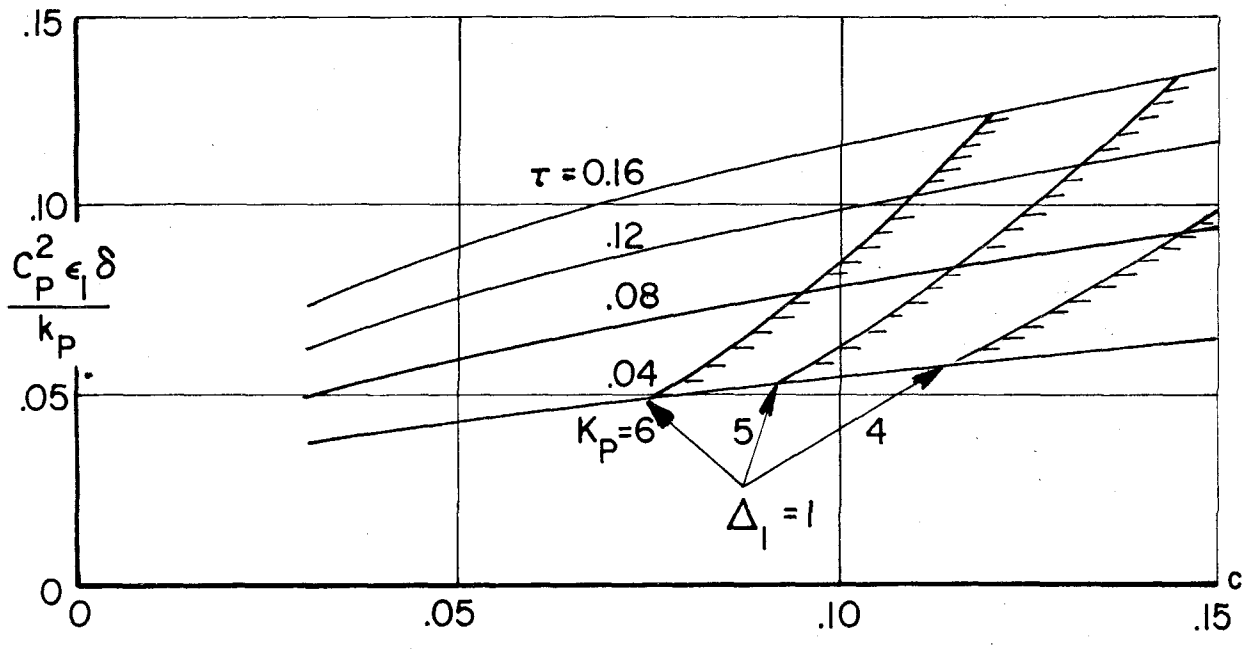

Figure 22. Optimum boundary layer thickness at choking in plane test section ($\gamma = 1.4$)

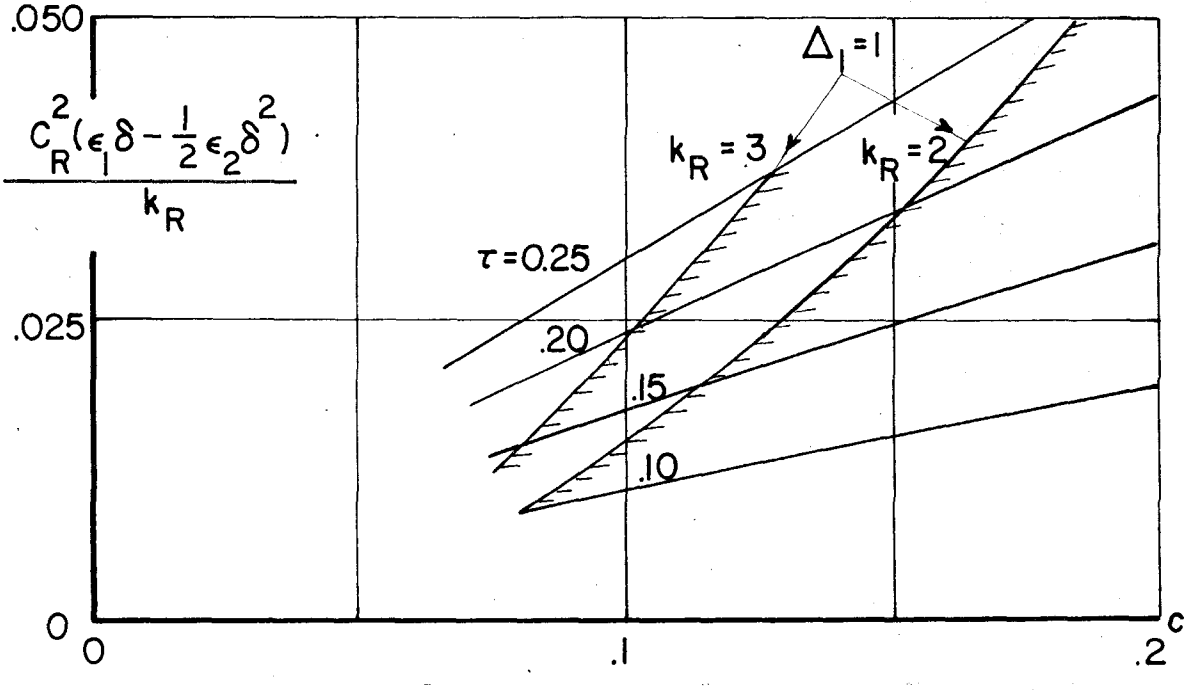

Figure 23. Optimum boundary layer thickness at choking in circular test section ($\gamma = 1.4$)